Extreme Temperature Regimes during the Cool Season: Recent Observed Behavior and Low Frequency Mode Modulation

A Thesis
Presented To
The Academic Faculty

by

Rebecca Marie Westby

In Partial Fulfillment
of the Requirements for the Degree
Master of Science in the
School of Earth and Atmospheric Sciences

Georgia Institute of Technology

December 2011

Extreme Temperature Regimes during the Cool Season: Recent Observed Behavior and Low Frequency Mode Modulation

Approved by:

Dr. Robert X. Black, Advisor
School of Earth and Atmospheric Sciences
Georgia Institute of Technology

Dr. Judith A. Curry
School of Earth and Atmospheric Sciences
Georgia Institute of Technology

Dr. Yi Deng
School of Earth and Atmospheric Sciences
Georgia Institute of Technology

Date Approved: November 10, 2011

For Elizabeth and Frederick Zimmer, who always encouraged me to dream big and reach for the stars.

Acknowledgements

I would like to acknowledge and extend my heartfelt gratitude to the following people who have made the completion of this thesis possible: my advisor, Dr. Robert X. Black, for patient guidance and support throughout the research and writing process, Dr. Yi Deng for providing valuable commentary and suggestions on this work, and Brad Hegyi for all the great discussions and ever-helpful assistance along the way. A special thanks also goes out to my family and friends, especially Toby Xu, for all their love, support and encouragement in the pursuit of my education.

Table of Contents

Page

List of Tables

Page

List of Figures

Page

List of Abbreviations

AO	Arctic Oscillation
AMO	Atlantic Multi-Decadal Oscillation
BKW	Belsley-Kuh-Welsh
CAO	cold air outbreak
CO	Cochrane-Orcutt
CPC	Climate Prediction Center
DW	Durbin-Watson
ENSO	El-Niño Southern Oscillation
ETR	extreme temperature regime
MERRA	Modern Era Retrospective-Analysis for Research and Applications
MW	Midwest
NAO	North Atlantic Oscillation
NCAR	National Center for Atmospheric Research
NCEP	National Centers for Environmental Prediction
NE	Northeast
NPGO	North-Pacific Gyre Oscillation
PDO	Pacific Decadal Oscillation
PNA	Pacific-North American pattern
SAT	surface air temperature
SE	Southeast
T	temperature
Twc	equivalent wind chill temperature
WW	warm wave

Summary

During the boreal cool season, regional climate in the United States is strongly impacted by extreme temperature regimes (ETRs), including both cold air outbreaks (CAOs) and warm waves (WWs), which have significant impacts on energy consumption, agriculture, as well as the human population. Using NCEP/NCAR and MERRA reanalysis data, the statistical characteristics of ETRs over three distinct geographical regions are studied: the Midwest (MW), Northeast Megalopolis (NE), and Deep South (SE). The regional long-term variability in the frequency and amplitude of ETRs is examined, and the modulation of these ETRs by low frequency modes is quantified.

ETR behavior is characterized using three different metrics applied to both T and Twc: 1) the number of extreme cold/warm days, 2) a seasonal cumulative "impact factor", and 3) a peak normalized anomaly value. A trend analysis reveals a significant downward trend in SE WW events from 1949-2011. Otherwise, no significant trends are found for ETRs in any of the other regions. Thus, these results indicate that there has not been any significant reduction in either the amplitude or frequency of CAOs over the United States during the period of analysis. In fact, for the SE region, the recent winters of 2009/2010 and 2010/2011 both rank among the top 5 in terms of CAO metrics. In addition, strong interannual variability in ETRs is evident from 1949-2011 in each region. Linear regression analysis is then used to determine the associations between ETR metrics and the seasonal mean state of several low frequency modes, and it is found that ETRs tend to be modulated by certain low frequency modes. For instance, in the SE region, there is a significant association between ETRs and the phase of the North Atlantic (or Arctic) Oscillation (NAO/AO), the Pacific North American (PNA) pattern (for WWs only), the Pacific Decadal Oscillation (PDO) and the El Niño-Southern Oscillation (for WWs only). Over

the MW region, WWs are modulated by the NAO/AO and PNA patterns, while in the NE region, the AO, NAO (for WWs only) and PDO (for WWs only) are implicated. In addition, it is found that there is an asymmetry between the low frequency mode modulation of CAOs and WWs. Multiple linear regression analysis is then used to quantify the relative roles of the various low frequency modes in explaining interannual variability in ETR metrics, and reveals that various combinations of low frequency modes can explain anywhere between 10% and 50% of the variance in the ETR metrics.

Chapter 1

Introduction

Extreme temperature regimes (ETRs), including cold air outbreaks (CAOs) and warm waves (WWs), during the boreal cool season affect regional economies and human safety over large portions of the United States via their significant impacts on energy consumption, local agriculture, and human health. A CAO event is characterized by an equatorward surge of polar air into the middle or lower latitudes (Walsh et al. 2001), while a WW event is characterized by a poleward surge of warm tropical air into the middle or high latitudes, and both of these events have the potential to severely disrupt human activities because of their rapid onset (Konrad and Colucci 1989).

The extremely cold temperatures associated with CAOs put humans at a higher risk of frostbite, hypothermia, and other cold-related health hazards, leading to approximately 30 deaths per year (Cellitti et al. 2006), while economic losses in the agriculture and transportation industries can cost billions of dollars due to crop damage, livestock death, and transportation delays (Celitti et al. 2006). Occasionally, the effects of these agricultural losses can last for several years, requiring a multiyear recovery period before production returns to pre-freeze levels (Rogers and Rohli 1991). Extremely cold temperatures also pose a threat to infrastructure if temperatures fall below the threshold for which buildings and other infrastructural components were designed (Vavrus et al. 2006). These potential impacts can be experienced in any region affected by a CAO; however, these impacts are especially harmful along the East and Gulf Coasts, where the majority of the population is less accustomed to extreme cold temperatures (Celitti et al. 2006).

Even though cool season WWs have historically received much less attention than CAOs, WWs can also have equally significant impacts. The abnormally warm temperatures associated with WWs causes rapid melting of snow and ice, leading to the ice damming and flooding of rivers and other bodies of water, and significant losses in the winter sports industry. Additionally, WWs pose an increased threat of frost damage to the agriculture industry because the warm temperatures associated with these events induce premature plant development, which is then halted by the return of colder normal conditions, often to the detriment to the plant (Gu et al. 2008). Therefore, both CAOs and WWs have the potential to impose significant impacts on the economy as well as the human population. Further research on the trends in the frequency and amplitude of ETRs and the associations of ETRs with various modes of the large-scale circulation can provide valuable scientific insight, leading to better forecasts of these events and subsequent mitigation of the negative impacts associated with ETRs.

One primary challenge in identifying ETRs is that there are no standardized definitions for either CAOs or WWs. Several different criteria have been used to identify CAOs in past studies, including the persistence of anomalously cold temperatures, high pressure, northerly winds, horticultural damage, or any combination of these, at a given location for a specified length of time (Wheeler et al. 2011). However, the particular definition used is typically dependent upon the focus of the research, the data available, and the nature of the event under study (Portis et al. 2006). In contrast to CAOs, the lack of a standardized definition for WWs is purely a result of the minimal body of literature on the subject. Nonetheless, the vast majority of traditional ETR definitions typically apply a local temperature anomaly criterion to identify events. This research expands this ETR definition to identify ETRs in terms of large amplitude anomalies in both temperature and wind chill. The motivation to also consider a wind chill

measure is driven by the recognition that the net impact of ETRs, particularly CAOs, on energy consumption and human exposure is not only a function of air temperature, but also depends on how quickly heat is transported away from local sources by wind. In addition, wind chill equivalent temperatures have been proven to reflect the human experience of cold and therefore can be a predictor of human sensations of cold temperatures (Osczevski and Bluestein 2005).

Previous research on CAOs found no evidence of any apparent trend toward fewer extreme cold events in the United States (Walsh et al. 2001 and Portis et al. 2006). However, no other studies have yet examined the most recent trends in CAO frequency over the United States. Therefore, one of the primary goals of this study is to expand upon the Walsh et al. (2001) and Portis et al. (2006) studies and examine trends in CAO frequency through the winter of 2011. Furthermore, this study will also include a new additional focus on the trends in frequency and amplitude of WWs during the boreal cool season. Curiously, despite not finding a trend in the frequency of CAOs, the Portis et al. 2006 study found an overall warming trend in mean winter temperatures since 1948. The warming trends were evident in both the high-latitude formation regions as well as the midlatitudes, and the warming trend in high-latitude formation regions has been confirmed by a recent study carried out by Hankes and Walsh (2011). However, this accompaniment of warming mean winter temperatures along with the lack of a decreasing trend in CAO frequency presents an intriguing paradox. This suggests, then, that there must be some other mechanism or process in the atmosphere that has a stronger impact on the interannual variability and trends in CAOs than the mean background temperature. One such mechanism could be the large-scale circulation.

The past two winters have been prime examples of this paradox. Both winters were exceptionally cold (Cohen et al. 2010, Guirguis et al. 2011, and Wang et al. 2010) despite having

some of the warmest mean winter temperatures on record (Cohen et al. 2010). The winter of 2009-2010 made headlines for its fierce snow storms and brutally cold temperatures in parts of the United States, while the winter of 2010-2011 was also anomalously cold and even more extreme for the majority of the United States (Guirguis et al. 2010). One important commonality between the past two winters was the persistence of the negative NAO, which reached unprecedented strength during the past two winters (Guirguis et al. 2010), and remained consistently below the previous 60-year average (Wang et al. 2010). Additionally, the seasonally (DJF) averaged AO, was the lowest observed since at least 1950 (Cohen et al. 2010). Therefore, based on these studies it appears that the large-scale circulation likely plays a key role in the fact that the trends in CAO frequency have not lessened over the past several decades.

Prior research has shown that on a per-event basis, regional ETRs, namely CAOs, are modulated by the large-scale low frequency modes of variability. For example, CAOs over central and eastern North America have been linked to the positive phase of the Pacific-North American (PNA) teleconnection pattern (Downton and Miller 1993, Vavrus et al. 2006, Cellitti et al. 2006, Rogers and Rohli 1991), in which the build-up of an upper-air ridge of western North America promotes a northwest-to-southeast flow and facilitates the transport of cold air masses from polar latitudes towards the equator (Vavrus et al. 2006). CAOs over much of the United States have also been linked to the North Atlantic Oscillation (NAO), or the regional counterpart of the Arctic Oscillation (AO), which is systematically negative in the period leading up to the CAO event (Walsh et al. 2001 and Cellitti et al. 2006). Unlike CAOs, however, little is currently known about the nature and low frequency mode modulation of WWs during the boreal cool season. Even though prior studies have established important relationships between the large-scale circulation of the atmosphere and ETRs, none of these studies have quantified the

relationships, which is of utmost importance for forecasting purposes. Therefore, another goal of this study is to expand on the current knowledge of low frequency modes and their modulation on ETRs by examining several of the most prominent low frequency modes and quantifying the role of these natural modes of low frequency variability in determining seasonal ETR behavior.

In summary, the present study has two main objectives: (1) to examine the long-term interannual and decadal variability in the frequency and amplitude of ETRs and (2) to determine and quantify how the behaviors in ETRs are modulated by low frequency modes, and both are pursued via statistical analyses of observational reanalysis data. First, a climatology of ETR frequency and amplitude using both temperature and wind chill equivalent temperature criterion are constructed to examine long-term variability in ETR behavior. Then, correlation and multiple linear regression analyses will be used to assess the regional ETR modulation by several prominent low frequency modes. The results of this study confirm prior findings on historical trends in CAOs, and also provide new information on recent trends in CAOs over the eastern United States as well as quantify the regional modulation of ETRs by prominent low frequency modes of natural variability.

The remainder of this thesis is organized as follows: Chapter 2 explains the data and methods used to identify ETRs and describes the statistical analyses used. The results of this research are then presented in Chapter 3. The results of the long-term trend and variability analysis are described first and are compared to the historical behavior of CAOs found by other studies for validation. Next, the results of the correlation analysis are presented, which identify the qualitative relationships between ETRs and low frequency modes. Then, the results of the multiple linear regression analysis are discussed, which quantify ETR modulation by low

frequency variability. Finally, Chapter 4 summarizes the primary conclusions of this research and suggests directions for future research.

Chapter 2

Data and Methods

The primary dataset used for the identification of ETRs in this research was the reanalysis data from the National Centers for Environmental Prediction – National Center for Atmospheric Research (NCEP/NCAR) (Kalnay et al. 1996). NCEP/NCAR is the longest reanalysis dataset currently available, and is therefore ideal for studying the long-term trends and variability of ETRs. The subset of data used for this analysis spans from January 1948 – February 2011, resulting in a 64-year analysis period. The variables from this dataset used for ETR identification in this analysis are the daily mean surface air temperature, daily mean u-wind and daily mean v-wind at the $\sigma = 0.995$ level, the closest available level to the surface, and have a grid resolution of 2.5° latitude x 2.5° longitude.

For comparison, a secondary dataset used for the identification of ETRs was from the National Aeronautic and Space Administration (NASA) Modern Era Retrospective-Analysis for Research and Applications (MERRA) (Suarez et al. 2008). This dataset is disseminated by the Global Modeling and Assimilation Office (GMAO) and the Goddard Earth Sciences Data and Information Services Center (GES-DISC). One of the primary benefits of this dataset is that it has a resolution of 1/2° latitude x 2/3° longitude, which is a higher resolution than that of the NCEP/NCAR reanalysis data. However, this dataset has a much shorter duration, and spans only from 1979-2011. Nonetheless, despite this shortened time span and the subsequent limitations on the utility of this particular dataset for determining long-term variability, it is beneficial to use this dataset to determine whether similar statistical results in identifying ETRs are found for both datasets over the period 1979-2011. The variables from this dataset used for ETR identification

in this analysis are the daily mean 2-m surface air temperature, daily mean 10-m u-wind and daily mean 10-m v-wind, which are comparable to the NCEP/NCAR variables used.

The indices used for the investigation of ETR modulation by low frequency modes were from the Climate Prediction Center (CPC) and were accessed via the Earth System Research Laboratory (ESRL) Physical Sciences Division (PSD) website (http://www.esrl.noaa.gov/psd/data/climateindices/). The primary low frequency modes of interest are the: North Atlantic Oscillation (NAO), Arctic Oscillation (AO), Pacific-North American Oscillation (PNA), the Pacific Decadal Oscillation (PDO), Multivariate ENSO (MEI), Nino 3.4, and the Southern Oscillation (SOI). These low frequency modes were chosen because most of them are known to impact surface air temperature over the regions of interest. The modulation of ETR behavior by the Atlantic Multi-Decadal Oscillation (AMO) (CPC) and the North Pacific Gyre Oscillation (NPGO) (http://www.o3d.org/npgo/) was also considered. For this analysis, the winter (DJF) mean index of each of these low frequency modes was used, which span from 1950-2011, except for the SOI and the NPGO, which span from 1951-2011.

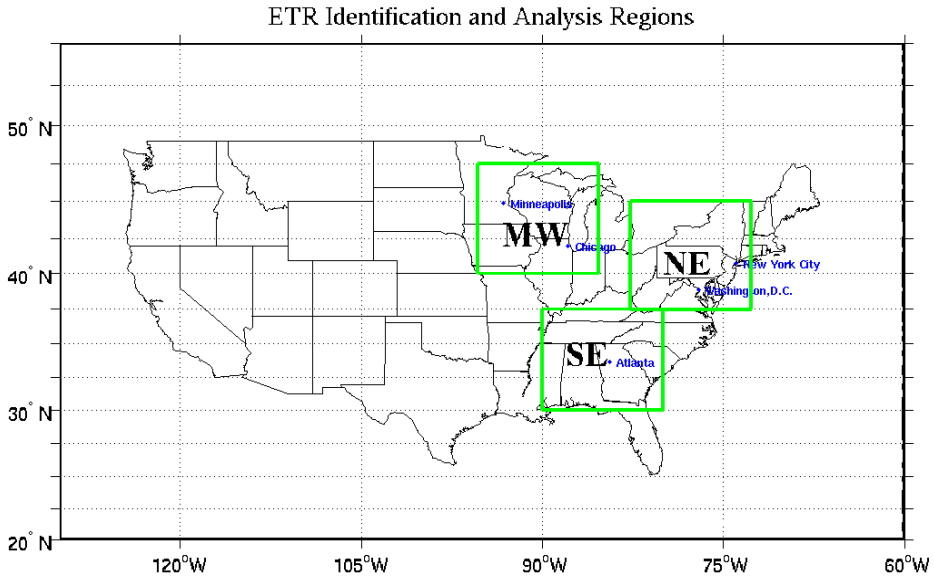

Figure 1: Extreme Temperature Regime Identification and Analysis Regions

Extreme temperature regimes were identified for three important geographical regions over the eastern United States: the Midwest (MW), the Southeast (SE), and the Northeast (NE). The Midwest was chosen because CAOs are frequent and therefore provides an important baseline for comparative analyses with past studies or other events. The Northeast region was also chosen because this region includes two large urban population centers, New York and Washington, D.C., which are also often affected by ETR events. And finally, the Southeast region was chosen because ETR events have been recognized to have significant impacts on the major urban centers as well as regional agriculture. The boundaries of the defined regions are shown in Figure 1 and are constrained by the resolution of the datasets used.

In this analysis, ETRs were identified using three different metrics dependent upon the regionally-averaged daily mean surface air temperature or equivalent wind chill temperature anomalies. The daily mean surface air temperature (T) is simply based off the measurement of temperature, while the daily mean equivalent wind chill temperature (Twc) is a function of both the daily mean surface air temperature and the daily mean wind speed. The equation for Twc is given in Equation 1 and follows the definition proposed by Osczevski & Bluestein (2005):

$$Twc = 35.74 + 0.6215T - 35.75V^{0.16} + 0.4275TV^{0.16} \quad (1)$$

where V is wind speed in mph and T is surface air temperature in degrees Fahrenheit. Before calculating the T and Twc anomalies, the daily mean temperature climatology was first constructed by calculating the areal average of T and Twc over each region for each day from January 1948-February 2011 and then computing the mean value of T and Twc for each calendar day across all 64 years. The daily mean temperature climatology was then smoothed using a Fourier analysis in which only the first six harmonics are retained. A comparison of the unsmoothed and Fourier-smoothed daily mean temperature climatologies for T and Twc in each

region are shown in Figures 2-4. The daily mean temperature climatologies for each region follow a similar pattern, reaching the lowest temperatures around mid-January and the highest temperatures near August, although the amplitudes of the temperature climatologies differ in each region. For instance, the temperature climatology in the SE region has the smallest amplitude, while the MW region has the largest amplitude. In addition, the daily mean temperature climatologies for Twc are generally similar to the daily mean temperature climatologies for T, as evidenced by Figures 2-4. However, the daily mean temperature climatologies for Twc have slightly larger amplitudes than for T. A similar process was then used to calculate and smooth the daily mean temperature standard deviation climatology. A comparison of the unsmoothed and Fourier-smoothed daily mean temperature standard deviation climatologies for T and Twc in each region are provided in Figures 5-7. The daily mean temperature standard deviation climatologies for each region follow a similar pattern, with the highest deviation from the mean occurring during the winter months (December-February) and the lowest deviation from the mean during the summer months (June-September), and are comparable in amplitude. Additionally, the daily mean temperature standard deviation climatologies for Twc are similar in pattern to those for T, although the standard deviation climatologies for Twc typically had slightly larger amplitudes.

Daily T and Twc anomalies were then obtained by subtracting the smoothed daily mean T or Twc climatology value from the regionally-averaged daily mean T or Twc. Several statistical characteristics of the resulting T' and Twc' distributions for DJF from 1948-2011 are shown in Table 1. First, the standard deviations of T' and Twc' in each region range from 9.5356 (SE T') to 13.4187 (MW Twc') and are comparable to the regional daily mean temperature standard deviation climatology values for DJF shown in Figures 5-7. In addition, the skewness of

T’ and Twc’ in each region, which measures the asymmetry of the anomaly values around the sample mean, ranges from -0.0066 (NE T’) to -0.3954 (MW Twc’). Compared to a Gaussian distribution, which has a skewness value of 0 by definition, the T’ and Twc’ distributions are all slightly negatively skewed. However, since the skewness values are relatively small and closer to 0 than to +1 or -1, these distributions can still be considered approximately symmetric or Gaussian for statistical purposes. Lastly, the kurtosis of T’ and Twc’ in each region, which measures how outlier-prone a distribution is, ranges from 2.6523 (MW T’) to 2.9600 (SE Twc’). The kurtosis of a normal distribution is 3, while a distribution with a kurtosis greater than 3 is more outlier-prone and has a distinct peak near the mean value, and a distribution with a kurtosis less than 3 is less outlier-prone and has a flat top near the mean rather than a sharp peak. However, since the kurtosis values in Table 1 do not differ greatly from 3, the T’ and Twc’ distributions can be considered to have a peak that resembles that of a normal distribution.

The anomalies were then normalized by dividing by the local Fourier smoothed daily mean temperature standard deviation climatology value. Therefore, the anomalies represent normalized departures from the daily normal T or Twc. One primary benefit of using normalized anomalies, rather than just the anomalies themselves, is that they allow the comparison of data from different time periods or locations. For example, in our analysis, T’ (Twc’) for one day is not strictly comparable to T’ (Twc’) on another day since T (Twc) itself is subject to a seasonal cycle. This issue is resolved by normalizing the daily temperature anomalies by the daily climatological standard deviation. Additionally, normalizing the anomalies allows for the objective categorization of extreme events and allows qualitative judgments to be made about the relative unusualness of particular values or events.

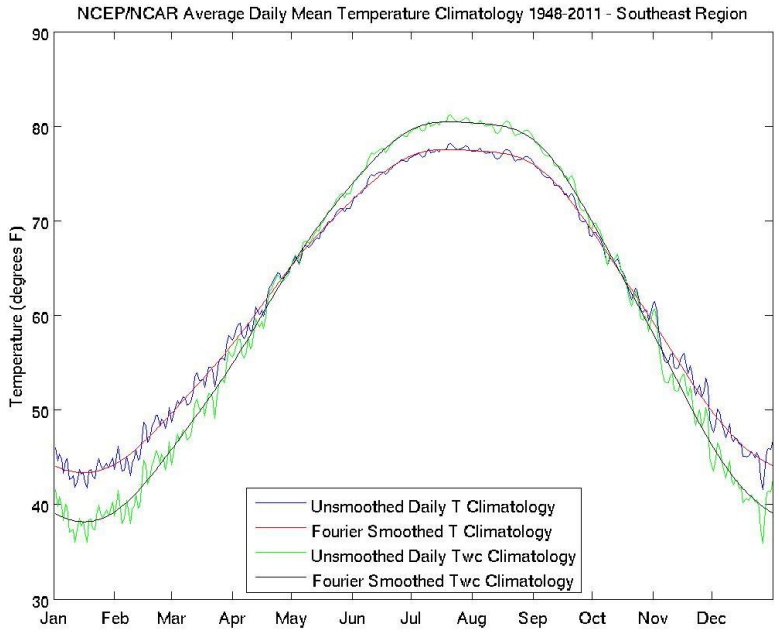

Figure 2: NCEP/NCAR Average Daily Mean Temperature Climatologies for the Southeast Region, 1948-2011

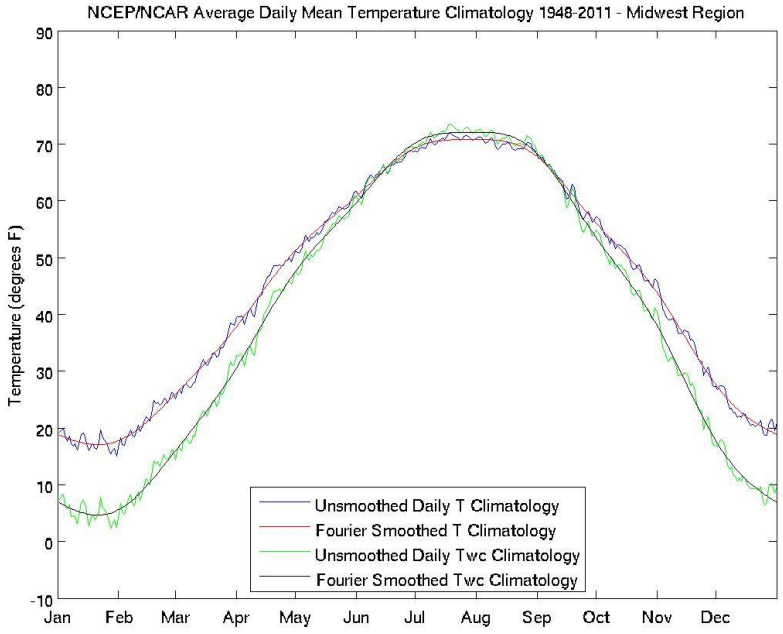

Figure 3: NCEP/NCAR Average Daily Mean Temperature Climatologies for the Midwest Region, 1948-2011

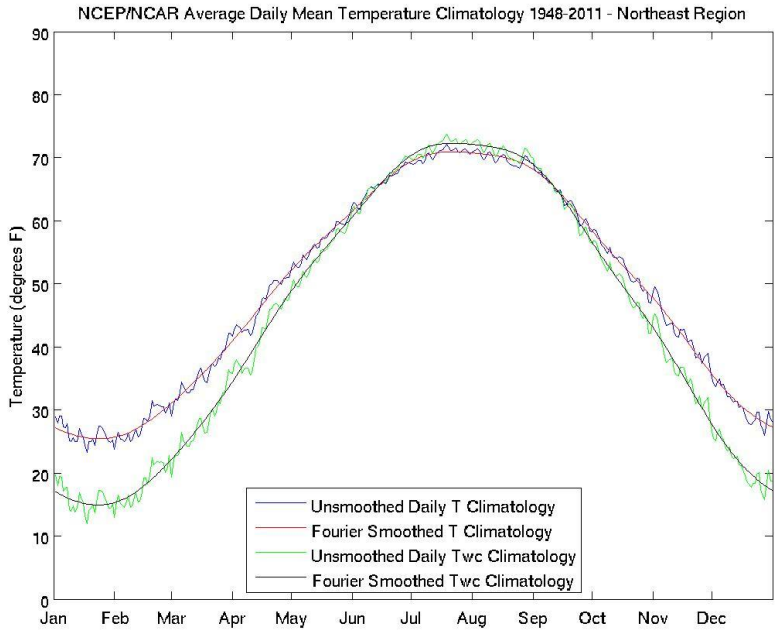

Figure 4: NCEP/NCAR Average Daily Mean Temperature Climatologies for the Northeast Region, 1948-2011

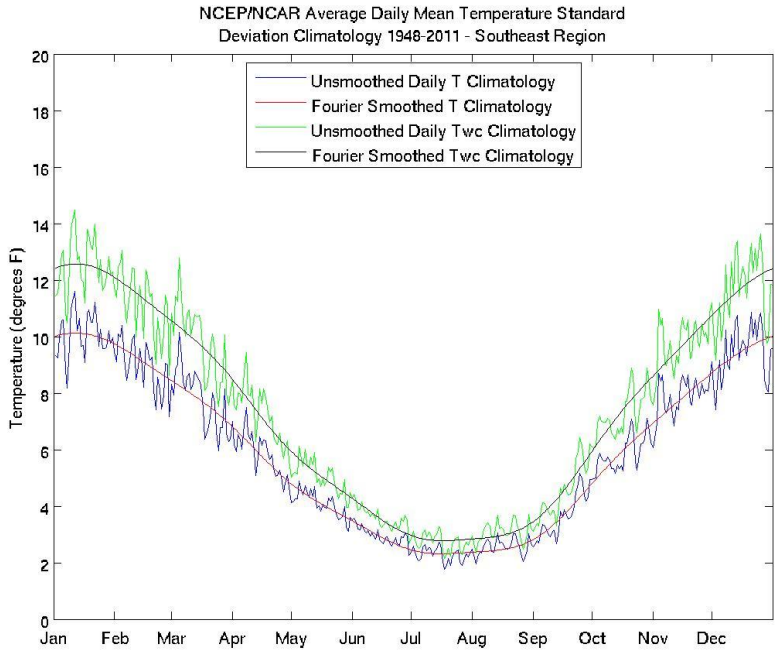

Figure 5: NCEP/NCAR Average Daily Mean Temperature Standard Deviation Climatologies for the Southeast Region, 1948-2011.

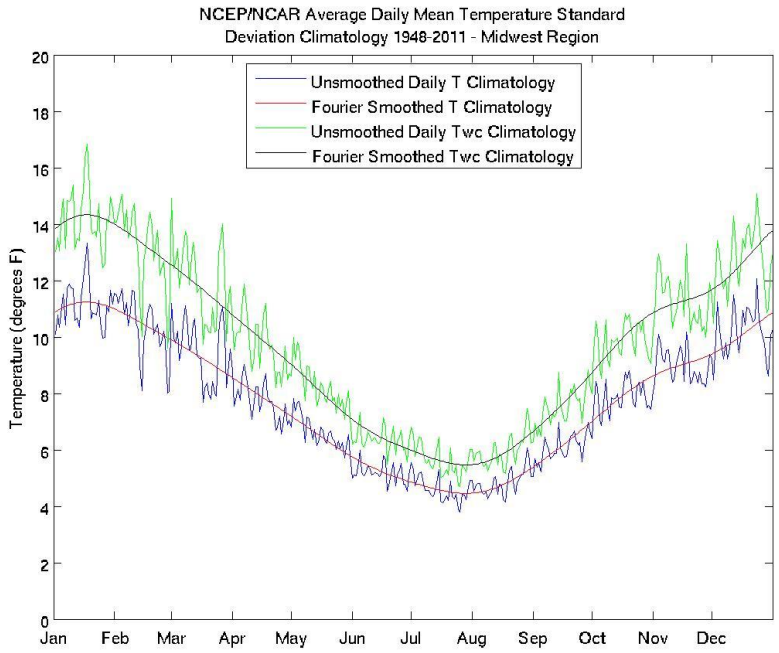

Figure 6: NCEP/NCAR Average Daily Mean Temperature Standard Deviation Climatologies for the Midwest Region, 1948-2011.

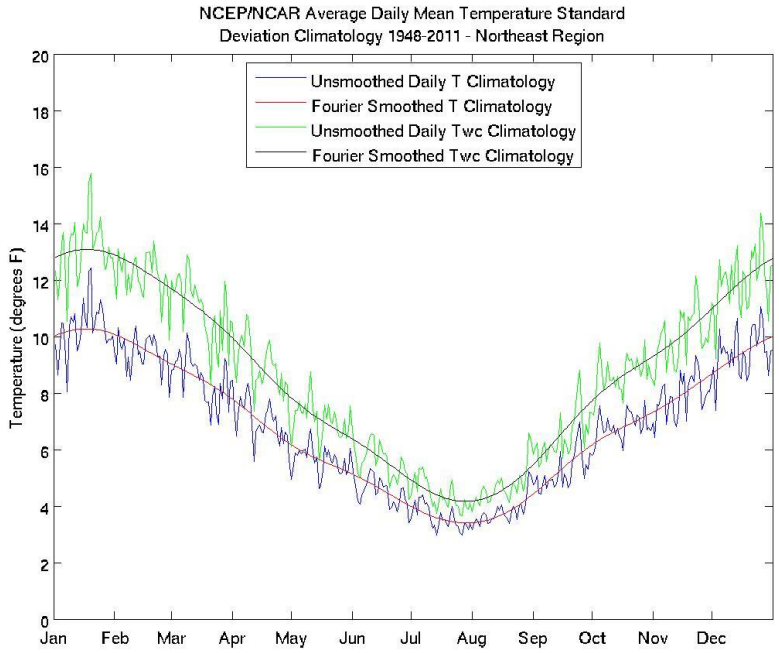

Figure 7: NCEP/NCAR Average Daily Mean Temperature Standard Deviation Climatologies for the Northeast Region, 1948-2011.

Table 1: Statistical Characteristics of the Temperature Anomalies, DJF 1948-2011

Region		Standard Deviation	Skewness	Kurtosis
MW	T'	10.5900	-0.2779	2.6523
	Twc'	13.4187	-0.3954	2.8264
SE	T'	9.5356	-0.2809	2.8052
	Twc'	11.8312	-0.3741	2.9600
NE	T'	9.7577	-0.0066	2.6794
	Twc'	12.4599	-0.1576	2.7340

However, care must also be used when using temperature anomalies to define ETR events because they are calculated relative to the daily mean temperature. If the daily mean surface air temperature changes over time, this could skew or mask the final results. Therefore, it is logical to investigate whether the daily mean surface air temperature changes over time. To test this, the daily mean temperature climatologies for the first and last 30 years of the NCEP/NCAR dataset were calculated for T and Twc for each region. The daily mean temperature climatologies for the first and last 30 years for the Southeast region are shown in Figure 8, and it is apparent that there is no systematic difference between these two periods. This was found to be true for both T and Twc for all regions of interest. Therefore, because no trend in the mean surface air temperature was found, the results of this analysis are are not influenced by a background trend in mean temperature. Additionally, the daily mean temperature standard deviation climatologies for the first and last 30 years of the dataset were calculated and examined to ensure that the variability in temperatures has also not changed over time (not shown). Again, no systematic difference was found between these periods for T or Twc in any region of interest.

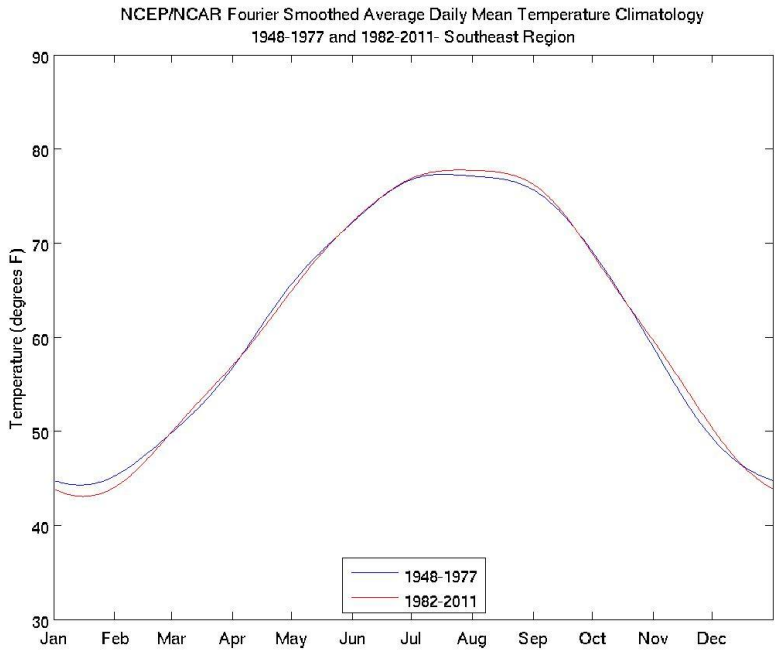

Figure 8: NCEP/NCAR Fourier Smoothed Average Daily Mean Temperature Climatology for the Southeast Region, 1948-1977 and 1982-2011

To further verify whether the statistical analyses will hold for this analysis, it is important to determine if the normalized temperature anomaly time series for each region also follows a Gaussian distribution. To verify this, histograms of the normalized T' anomalies for DJF from 1948-2011 for each region were plotted and overlaid with an equivalent Gaussian PDF (μ=0, σ=1) and are shown in Figures 9, 10, and 11. In general, there is good correspondence between the histogram of the normalized T' (blue bars) and the Gaussian PDF (red line) in each region. The NE region histogram (Figure 11) shows a near-perfect fit with the Gaussian PDF, while the MW (Figure 9) and SE (Figure 10) region histograms appear to have a slight skew. The skewness values for the MW, SE, and NE regions are -0.2786, -0.2680, and -0.0064, respectively. Thus, the histograms in each region are slightly negatively skewed. However, since these skewness values are relatively small and closer to 0 than to +1 or -1, the normalized temperature anomaly distributions are considered approximately symmetric, and therefore, the

statistical analysis results will be valid. In addition, it is assumed that the normalized Twc' also follows a Gaussian distribution due to the similarities observed thus far between T' and Twc'.

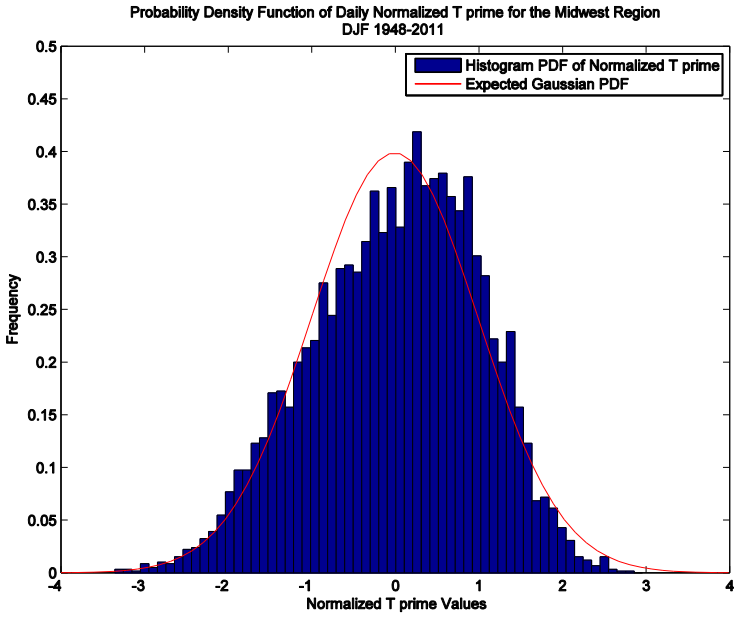

Figure 9: Probability Density Function of the Daily Normalized T' for the Midwest Region, DJF 1948-2011

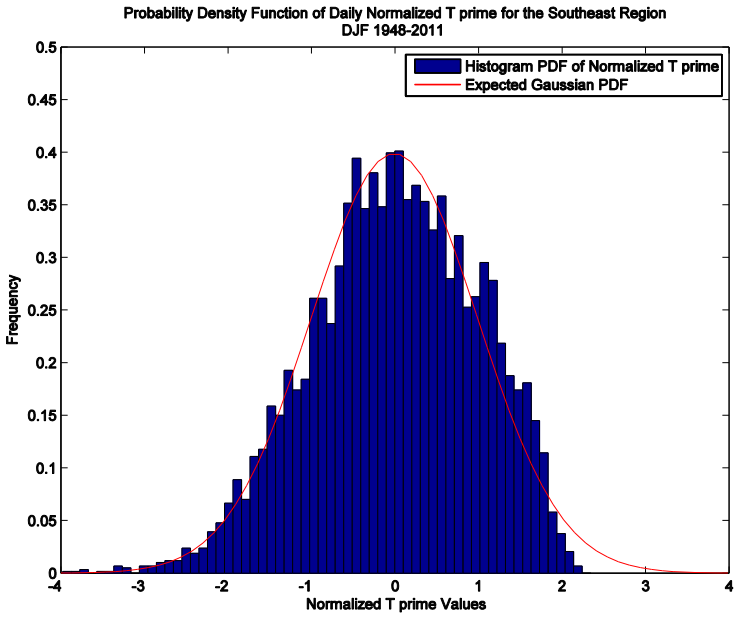

Figure 10: Probability Density Function of the Daily Normalized T' for the Southeast Region, DJF 1948-2011

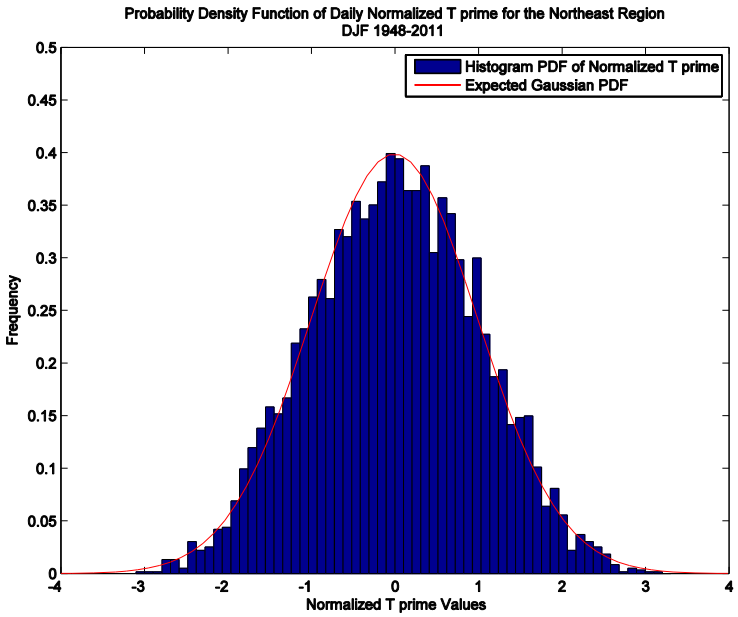

Figure 11: Probability Density Function of the Daily Normalized T' for the Northeast Region, DJF 1948-2011

To characterize the behavior of ETRs, three different metrics using T' and Twc' were devised. The first metric was the number of days per winter that T' or Twc' was above +nσ (defined as a warm event occurrence) or below –nσ (defined as a cold event occurrence), where n=1, 1.5, or 2 and the winter seasons are December – February and are labeled by the year of their January-February. The second metric was the impact factor of warm or cold days per season, which quantifies the cumulative effect of all the warm or cold days per winter season. This metric is calculated by summing the absolute values of the normalized T' or Twc' values for all days during the winter season exceeding the threshold +nσ or –nσ (where again n=1, 1.5, or 2), and is mathematically expressed in Equation 2.

$$\text{Impact Factor} = \sum_{n=1}^{\#\ of\ Qualifying\ Days} \frac{|T' or\ Twc'|}{\sigma} \qquad (2)$$

The third and final metric was the peak value per season, which was identified by finding the single largest magnitude of T' and Twc' for warm days and cold days in each winter season. The number of days metric will be used to represent the frequency of ETRs, while the impact factor

and peak value metrics will be used to represent the intensity of ETRs. While alternative definitions could have been used to identify ETRs, the results from this analysis should apply regardless of the exact criteria used based on the success of other studies that used temperature anomalies to define events. Additionally, these definitions of ETRs provide several desirable properties: (1) the first two metrics are able to easily identify different categories of ETRs, (2) these definitions provide a large sample size, which is required for the assessment of statistical significance (3) they do not constrain the behavior of ETRs to be spatially or temporally uniform, which is often required by percentile thresholds, (4) these definitions relate ETRs to easily and accurately measureable meteorological variables (average temperature and wind speed), (5) they allow for the distinction between warm events and cold events during the winter, and (6) they can be applied to assess ETRs based on current climate conditions or future climate conditions.

One of the main objectives of this study is to examine the trends in frequency and amplitude of ETRs, which are evaluated by correlating the time series of each ETR metric with time using linear regression, for the period 1949-2011. This analysis period is one year shorter than the full reanalysis dataset to account for the fact that the ETR metrics for 1948 do not represent a full seasonal assessment of ETRs since they do not include data for December 1947. All trends are accompanied with a p-value for occurrence by chance, which is calculated using a two-tailed Student's-t test. Trends are considered significant when the p-value is less than 0.05.

The second objective of this study is to determine and quantify how the interannual variability in ETRs is modulated by low frequency modes. First, correlation analysis is used to determine the association between each of the ETR metrics and the seasonal mean state of several prominent low frequency modes that are known or suspected to be associated with ETRs. However, this analysis was conducted for a slightly shorter period, from1950-2011, based on the

availability of the low frequency mode indices. The significance of these correlations was tested using a Student's-t test, and the correlations were considered significant if the p-value was less than 0.05 and marginally significant if the p-value was less than 0.10. Additionally, the effect of autocorrelation in the time series was accounted for by computing the effective degrees of freedom using the procedure of Wilks (2006). This ensures that the statistical significance of the correlations is not over-estimated due to autocorrelation in the time series.

Next, a multiple linear regression analysis was performed using the significantly correlated low frequency mode indices as predictor variables to quantify the relative roles of the various low frequency modes in explaining interannual variability in the ETR metrics, and to determine how much of the variance in ETR metrics can be attributed to each of the low frequency modes. Additionally, the use of multiple linear regressions allows for the quantification of simultaneous influences of multiple low frequency modes on the occurrence, frequency, and amplitude of ETRs. The general multiple linear regression equation used is given by Equation 3.

$$y = \beta_0 + \beta_1 x_1 + \beta_2 x_2 + \beta_3 x_3 + \cdots + \beta_n x_n \quad (3)$$

To determine which predictor or combination of predictors provides the best estimate for each of the ETR metrics, linear regressions were performed separately for each significantly correlated low frequency mode, as well as for each possible combination of significantly correlated low frequency modes. After all the regressions were completed, the statistics for each case or combination were examined, and the best set of predictors was determined to be the regression equation that had statistically significant regression coefficients as well as the highest possible r-squared value. However, when using multiple linear regressions, one must be aware of multicollinearities among the predictors because in many cases it isn't known a priori if one

predictor contains redundant information about another predictor. In this analysis, the predictors were tested for multicollinearity using the Belsley, Kuh and Welsch (BKW) variance-decomposition method (Belsley, Kuh and Welsch 1980). If multicollinearities were detected, only one of the multicollinear predictors was used in the regression. Additionally, the regression of the best set of predictors was tested for autocorrelation in the residuals via the Durbin-Watson (DW) test because autocorrelation in the residuals degrades the regression and its associated statistics. If there was autocorrelation in the residuals, then the multiple linear regressions were re-performed using the Cochrane-Orcutt (CO) method, which corrects for the artificially high confidence in the correlations that results from the autocorrelation, and accordingly, provides a more accurate statistical significance assessment. Finally, the variance explained was calculated by correlating the original ETR metric time series with the estimation of the time series produced by the best multiple linear regression and then squaring the correlation coefficient. This value represents the portion of the interannual variability in the ETR metric that is accounted for by that particular combination of predictors and provides a measure of how well future values in ETR metrics are likely to be predicted.

Chapter 3

Results and Discussion

This section will (1) examine the regional long-term variability in the frequency and amplitude of ETRs and (2) determine and quantify the how these behaviors in ETRs are modulated by several prominent low frequency modes. As described in Chapter 2, the analysis was carried out using both T' and Twc' criterion. However, as will be shown in Section 3.1, the results using T' and Twc' are virtually identical. Therefore, Sections 3.2 and 3.3 present and discuss the results using T' only. Additionally, note that the correlation analyses and multiple linear regression analyses were performed only for ETRs exceeding a threshold of $\pm 1\sigma$, and have yet to be investigated for thresholds of $\pm 1.5\sigma$ and $\pm 2\sigma$.

3.1 Regional Long-Term Variability Analysis

The regional long-term trend analysis for the number of WW days in the SE region reveals a statistically significant downward trend (at the 95% confidence level) in SE WW days above $+1\sigma$ from 1949-2011 (Figure 12). A statistically significant decreasing trend was also found for SE WW days above $+1.5\sigma$ (Figure 13), whereas the trend for SE WW days above $+2\sigma$ was not statistically significant (not shown). Interestingly, the results for T' and Twc' in Figures 12 and 13 are almost identical; therefore, several of the subsequent figures display T' results only. The impact factor trend analysis for SE WW days also found a statistically significant decreasing trend for days above $+1\sigma$ (Figure 14) and $+1.5\sigma$ (not shown), while no significant trends were present in the peak value trend analysis for SE WW days (Figure 15 shows the

results for days above +1σ). In addition, the time series in Figures 12-15 are characterized by relatively large year-to-year fluctuations, whether a statistically significant long-term trend exists or not. Thus, it is evident that WWs in the SE region tend to exhibit strong interannual variability in addition to a downward trend. In comparison, the trend analyses for the number of WW days above +1σ and +1.5σ and the impact factor for days above +1σ for the MW region (Figures 16-18, respectively) indicate a slight increase in WWs, while the peak value trend analysis for days above +1σ shows a small decrease in WWs (Figure 19). However, none of these trends, or those at any of the other threshold levels, were found to be statistically significant. Additionally, similar to the SE region findings, the results for T' and Twc' in the MW are almost identical (Figures 16 and 17) and the time series in Figures 16-19 show strong variability from year to year. In the NE region, the trend analyses for the number of WW days above +1σ and +1.5σ and the impact factor for days above +1σ (Figures 20-22, respectively) indicate a decrease in WWs, while the peak value trend analysis for days above +1σ shows a slight increase in WWs (Figure 23). Again, none of these trends, or those at any of the other threshold levels, were found to be statistically significant. Also, similar to the results in the SE and MW regions, the results for T' and Twc' in the NE are nearly indistinguishable (Figures 20 and 21) and the time series in Figures 20-23 vary strongly on a yearly basis. Overall, therefore, these results indicate that there has been a reduction in the frequency and amplitude of boreal cool season WWs over the SE US from 1949-2011, while no significant changes in WW behavior have occurred in the MW and NE regions. In addition, it is also evident that WWs in each region exhibit strong interannual variability.

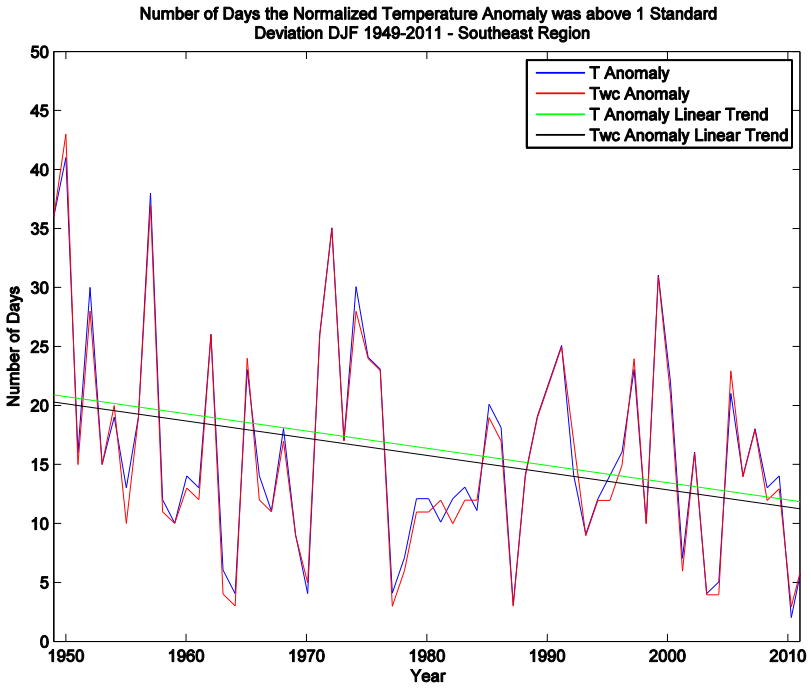

Figure 12: Number of Days the Normalized Temperature Anomaly was above +1σ for the Southeast Region, DJF 1949-2011

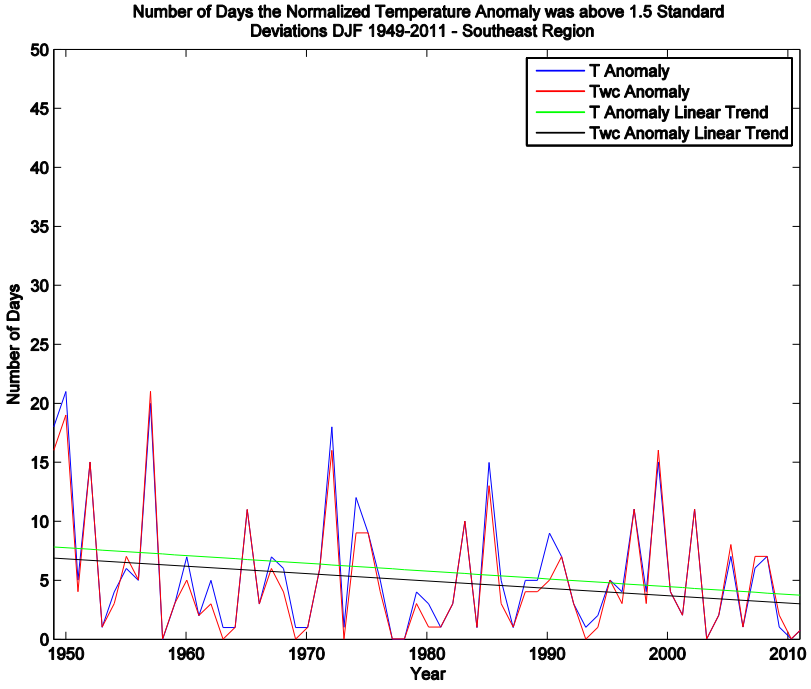

Figure 13: Number of Days the Normalized Temperature Anomaly was above +1.5σ for the Southeast Region, DJF 1949-2011

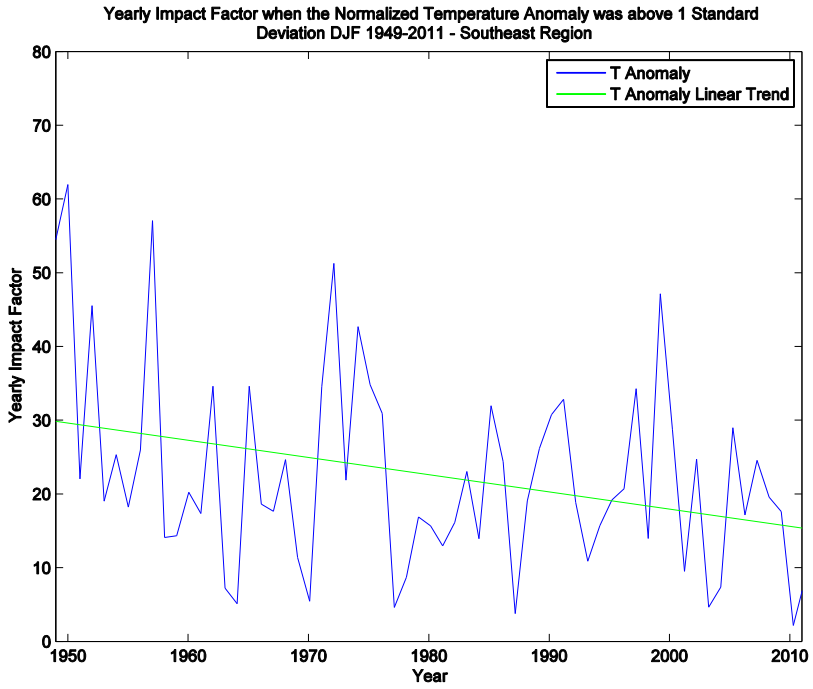

Figure 14: Impact Factor for Days the Normalized T' was above +1σ for the Southeast Region, DJF 1949-2011

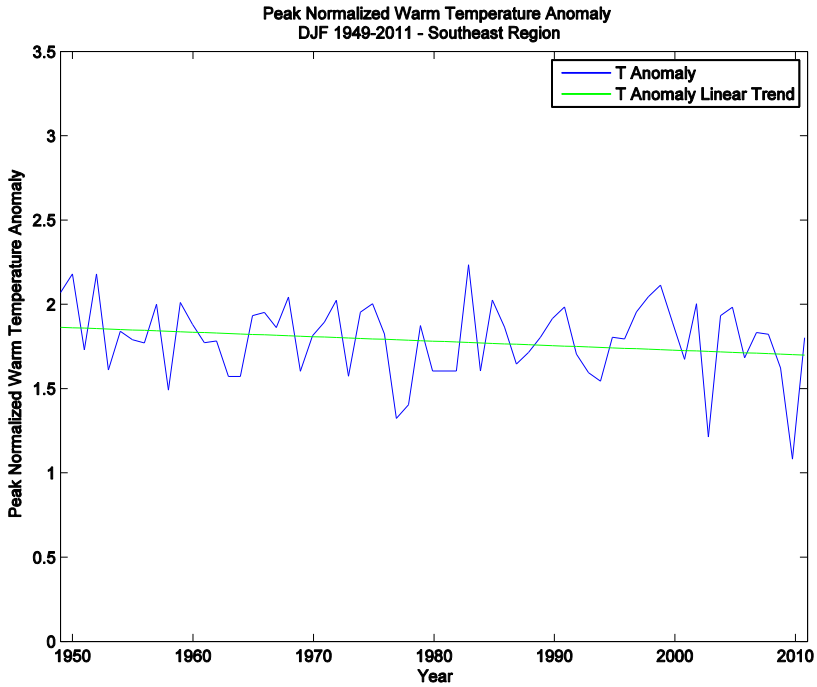

Figure 15: Peak Value for Days the Normalized T' was above +1σ for the Southeast Region, DJF 1949-2011

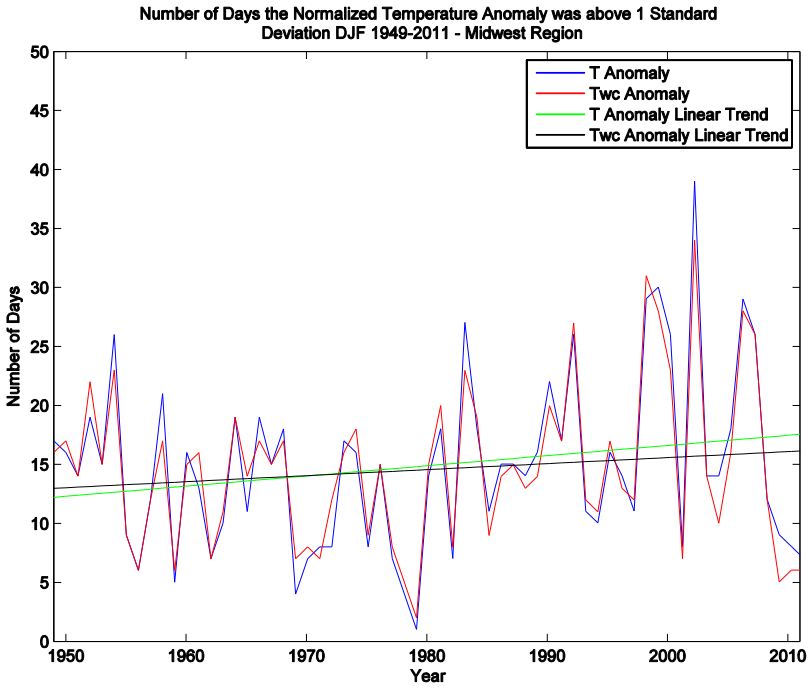

Figure 16: Number of Days the Normalized Temperature Anomaly was above +1σ for the Midwest Region, DJF 1949-2011

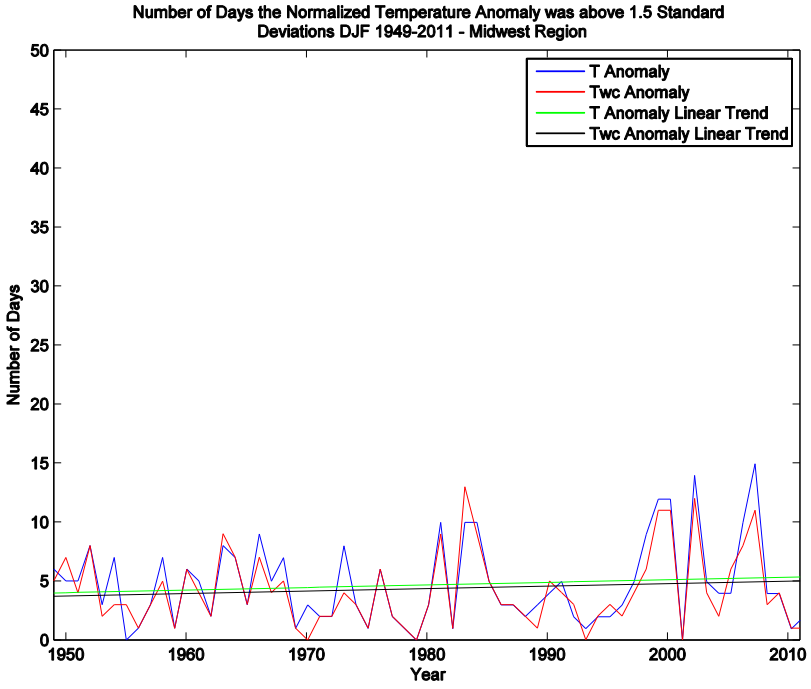

Figure 17: Number of Days the Normalized Temperature Anomaly was above +1.5σ for the Midwest Region, DJF 1949-2011

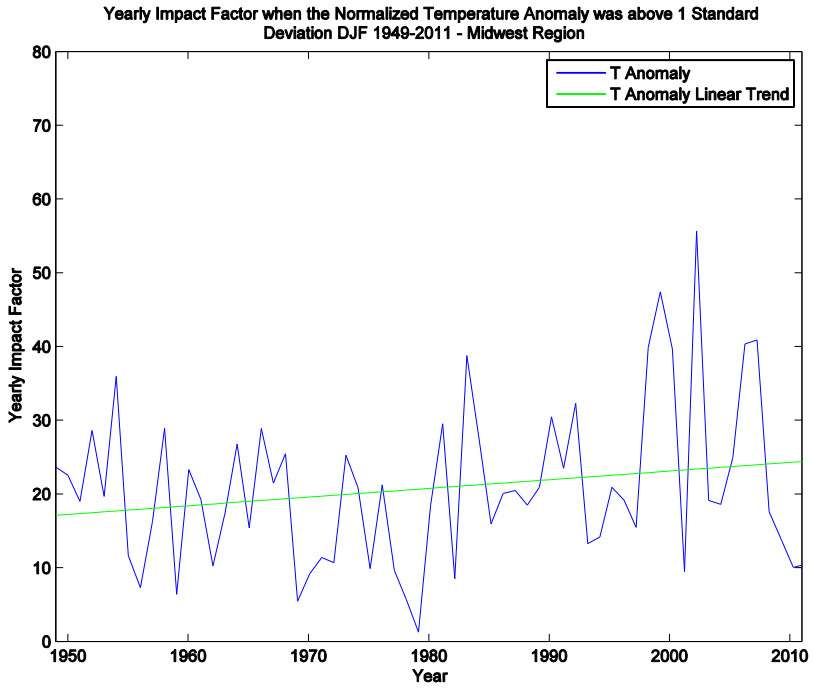

Figure 18: Impact Factor for Days the Normalized Temperature Anomaly was above +1σ for the Midwest Region, DJF 1949-2011

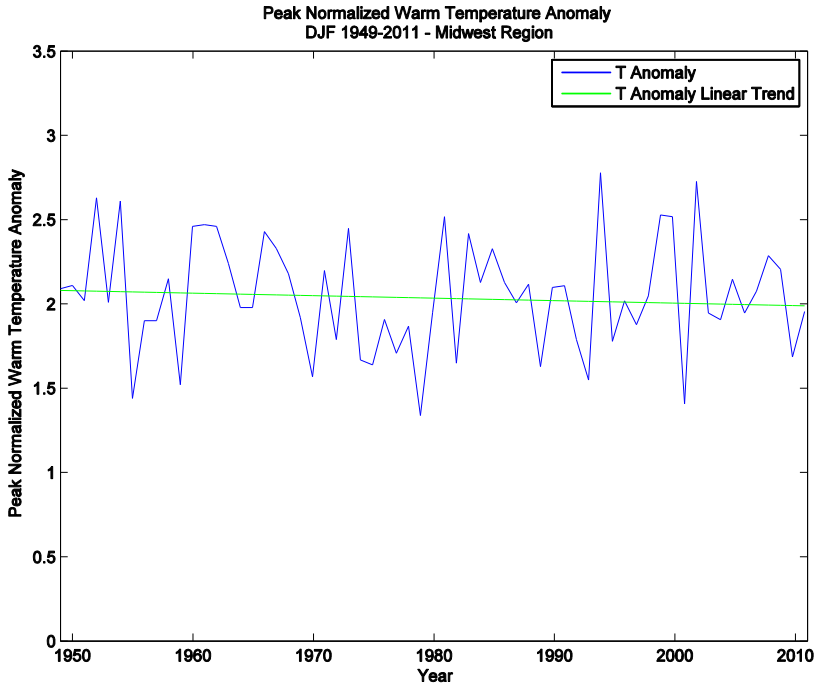

Figure 19: Peak Value for Days the Normalized Temperature Anomaly was above +1σ for the Midwest Region, DJF 1949-2011

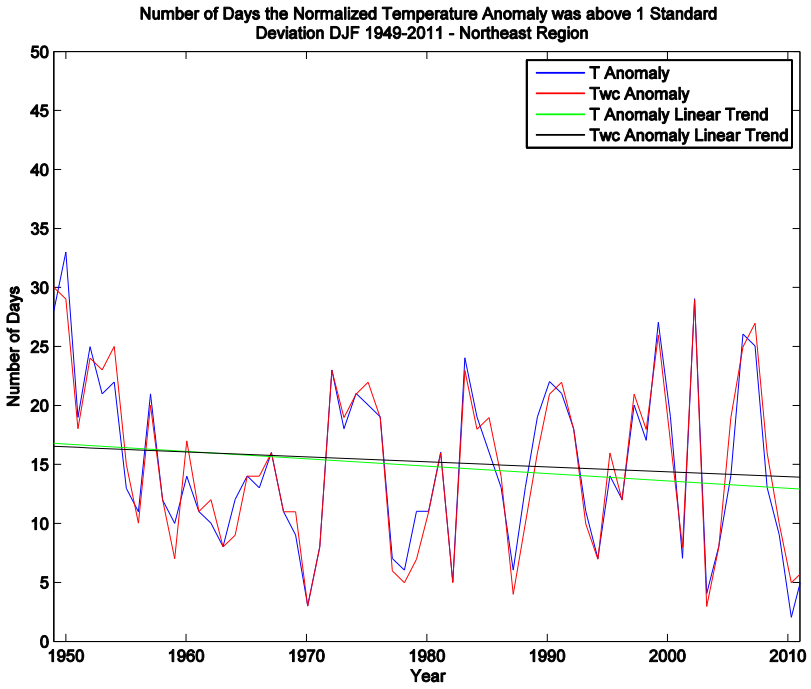

Figure 20: Number of Days the Normalized Temperature Anomaly was above +1σ for the Northeast Region, DJF 1949-2011

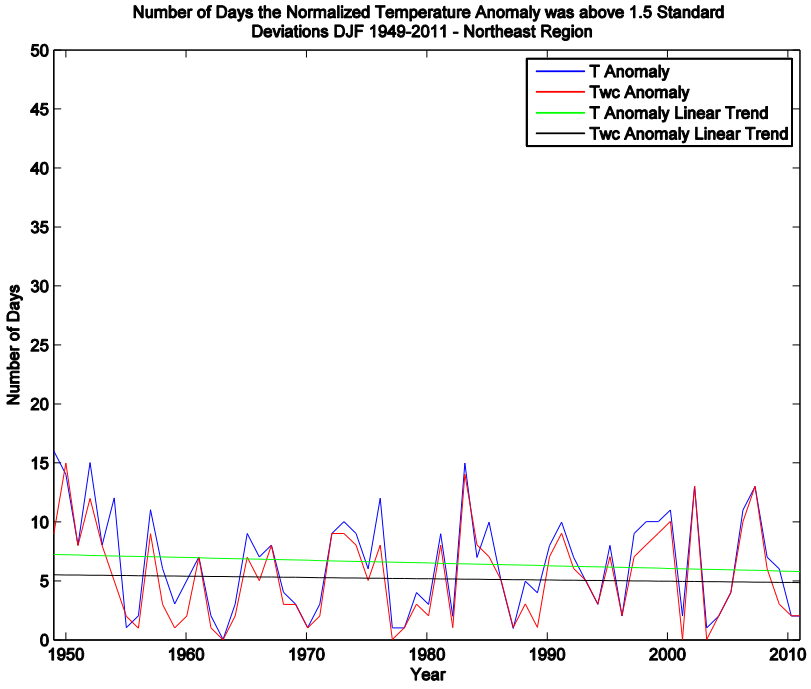

Figure 21: Number of Days the Normalized Temperature Anomaly was above +1.5σ for the Northeast Region, DJF 1949-2011

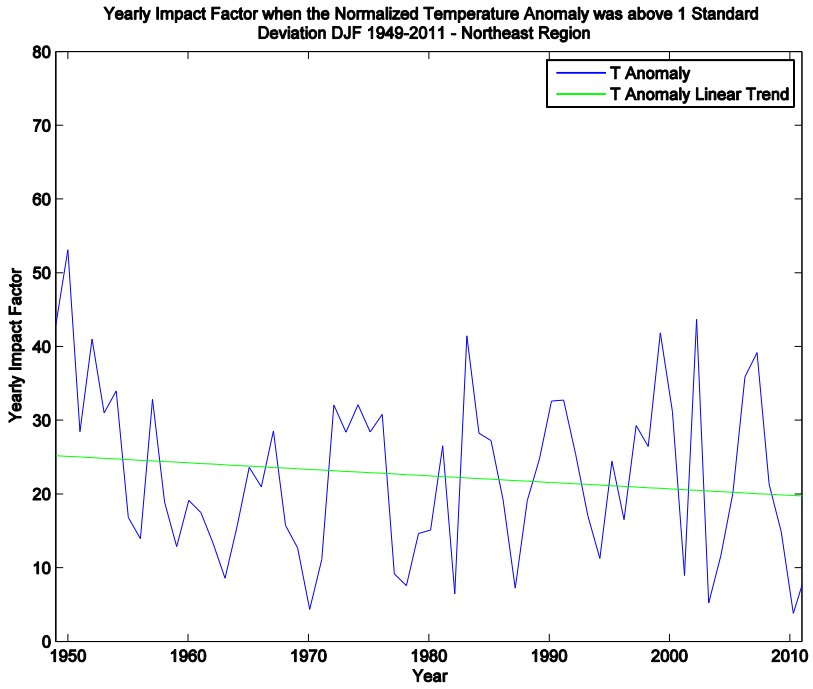

Figure 22: Impact Factor for Days the Normalized Temperature Anomaly was above +1σ for the Northeast Region, DJF 1949-2011

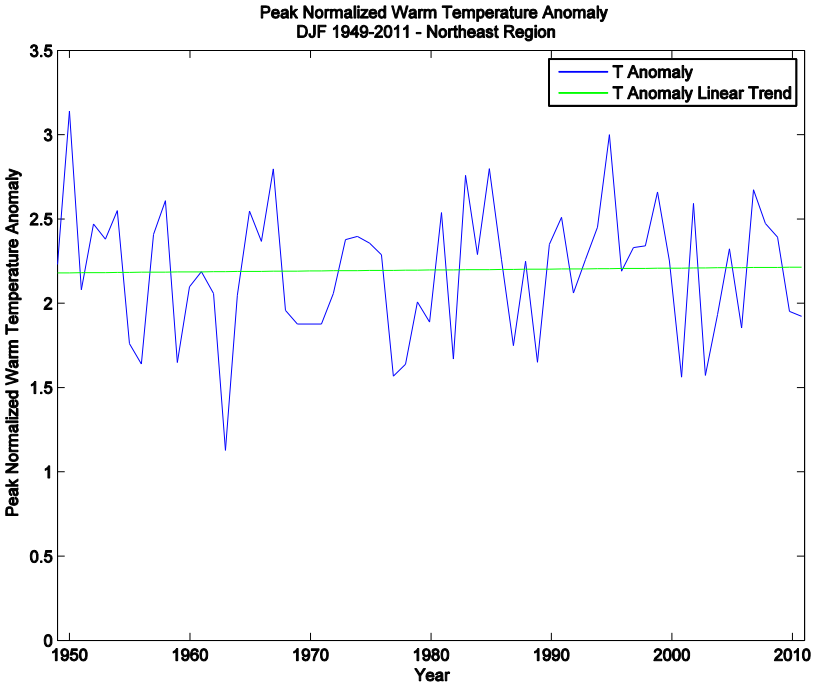

Figure 23: Peak Value for Days the Normalized Temperature Anomaly was above +1σ for the Northeast Region, DJF 1949-2011

The parallel results for CAOs are presented in Figures 24-35. As was the case with WWs, the results for T' and Twc' are almost identical (Figures 24-25, 28-29, and 32-33). It is also evident that CAOs, like WWs, exhibit strong interannual variability (Figures 24-35). Furthermore, the trend analyses for the number of days below -1σ and -1.5σ, the impact factor for days below -1σ, and the peak value trend analysis for days below -1σ for the SE region (Figures 24-27) all suggest an increase in CAOs. In comparison, the trend analyses for the number of days below -1σ and -1.5σ and the impact factor for days below -1σ for the MW and NE regions (Figures 28-30 and Figures 32-34, respectively) indicate a slight decrease in CAOs, while the peak value trend analysis for days below -1σ shows a small increase in CAOs (Figures 31 and 35, respectively). However, none of these trends, or any of those at any other threshold level, were found to be significant. Therefore, it can be broadly concluded that there has *not* been any significant reduction in either the amplitude or frequency of boreal cool season CAOs over the eastern United States from 1949-2011. These results confirm the findings of Walsh et al. (2001) and Portis et al. (2006), both of whom also found that there has been no apparent trend in CAO frequency since 1948. However, the results of the impact factor and peak amplitude trend analyses contradict the finding by Portis et al. (2006) that long-term CAO intensity trends vary spatially, where CAO intensity trends have decreased along the eastern seaboard and increased over the Midwest. As previously mentioned, the present analysis found that there have *not* been any significant trends in the impact factor or peak amplitude of CAOs from 1949-2011 for any of the three regions of interest. Therefore, these results additionally imply that the long-term trends of CAO intensity do not vary spatially.

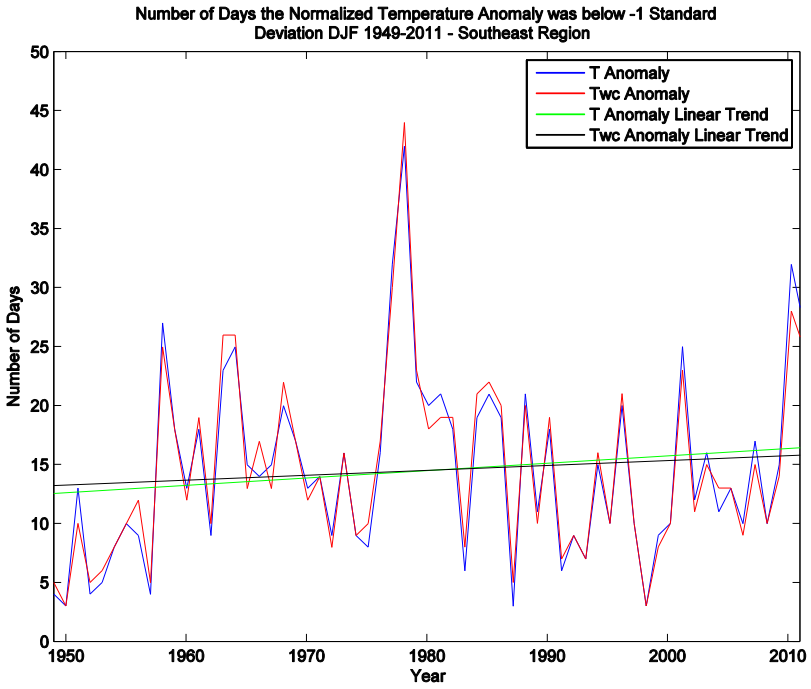

Figure 24: Number of Days the Normalized Temperature Anomaly was below -1σ for the Southeast Region, DJF 1949-2011

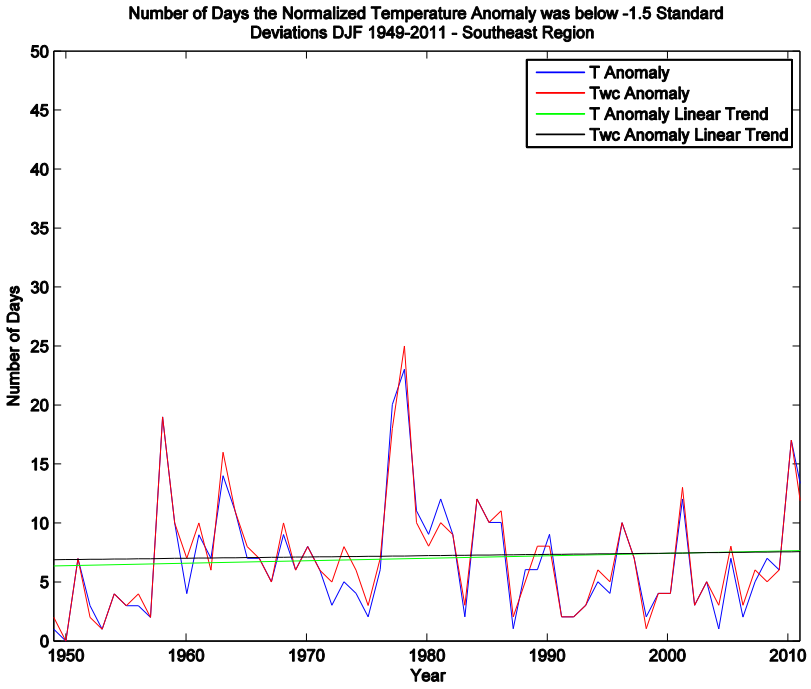

Figure 25: Number of Days the Normalized Temperature Anomaly was below -1.5σ for the Southeast Region, DJF 1949-2011

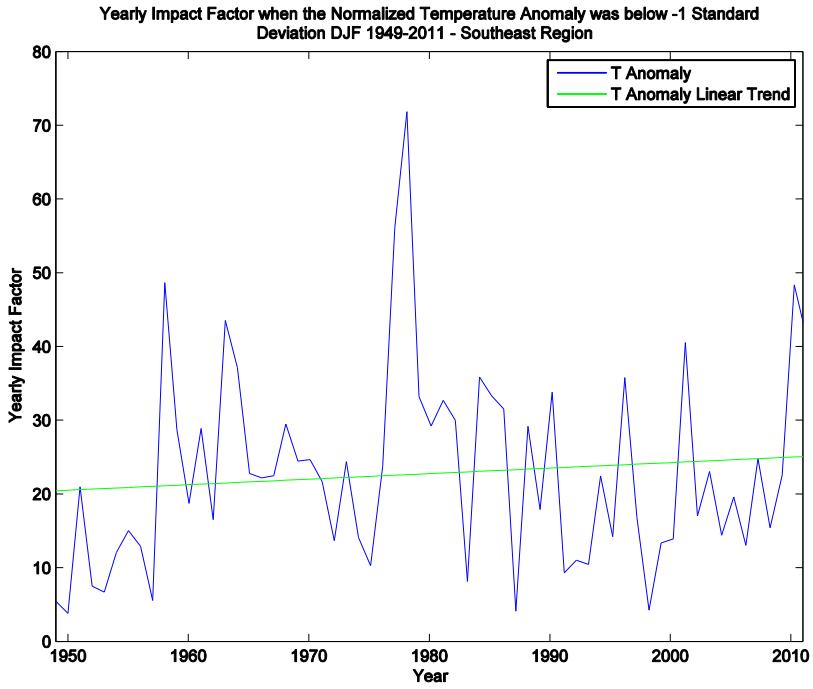

Figure 26: Impact Factor for Days the Normalized Temperature Anomaly was below -1σ for the Southeast Region, DJF 1949-2011

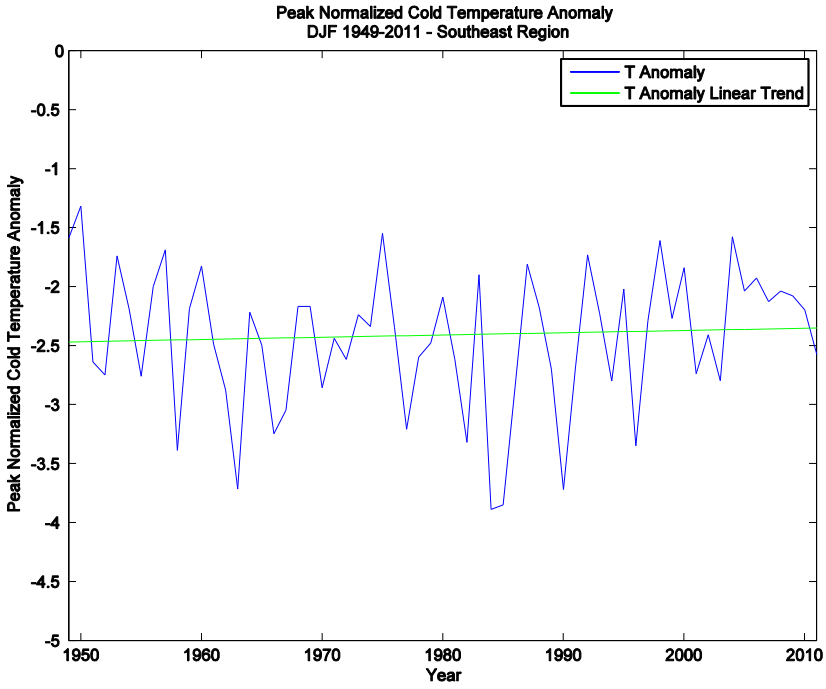

Figure 27: Peak Value for Days the Normalized Temperature Anomaly was below -1σ for the Southeast Region, DJF 1949-2011

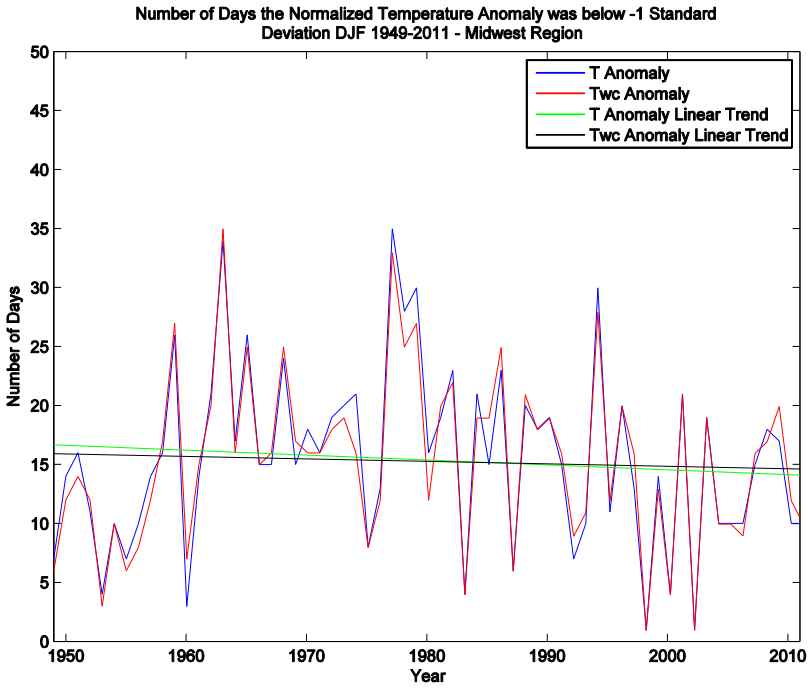

Figure 28: Number of Days the Normalized Temperature Anomaly was below -1σ for the Midwest Region, DJF 1949-2011

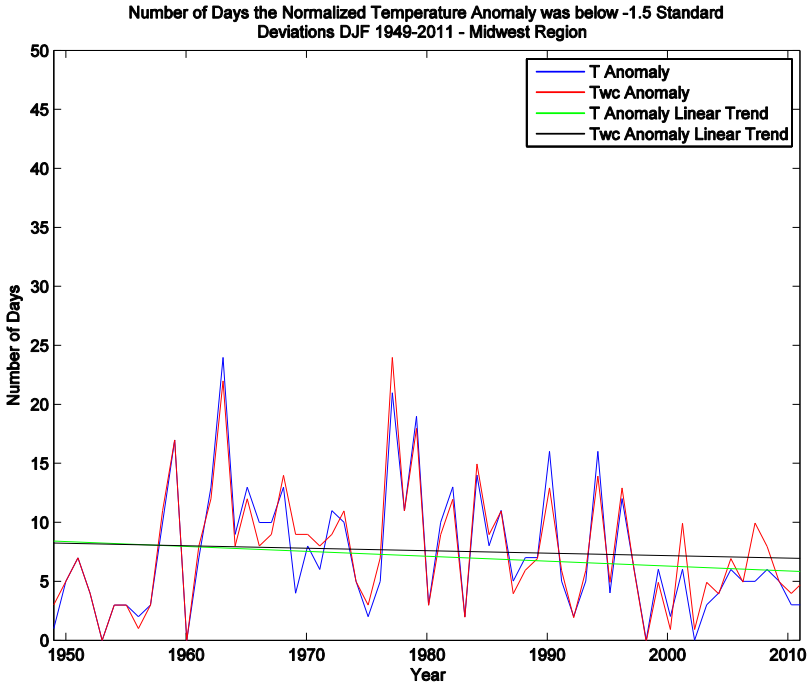

Figure 29: Number of Days the Normalized Temperature Anomaly was below -1.5σ for the Midwest Region, DJF 1949-2011

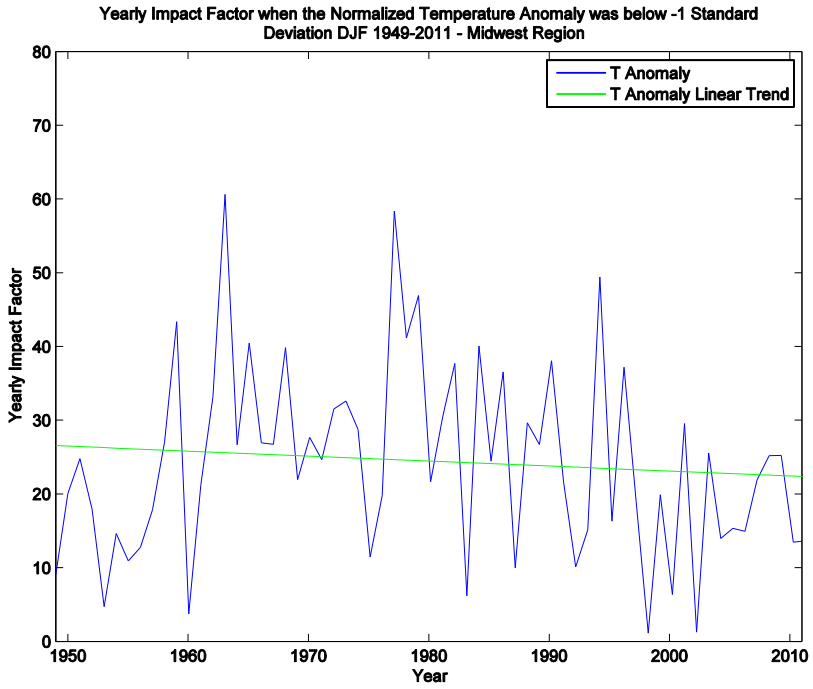

Figure 30: Impact Factor for Days the Normalized Temperature Anomaly was below -1σ for the Midwest Region, DJF 1949-2011

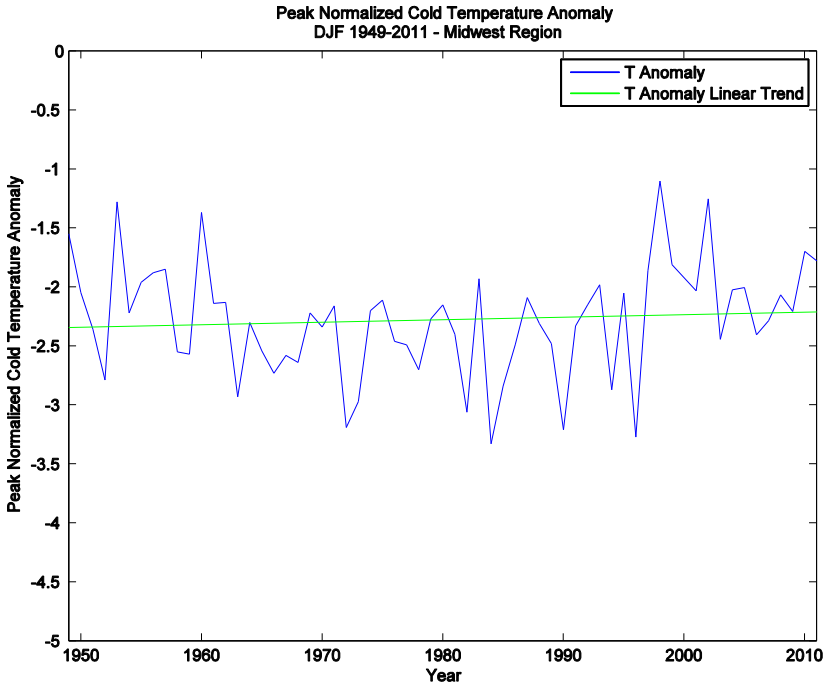

Figure 31: Peak Value for Days the Normalized Temperature Anomaly was below -1σ for the Midwest Region, DJF 1949-2011

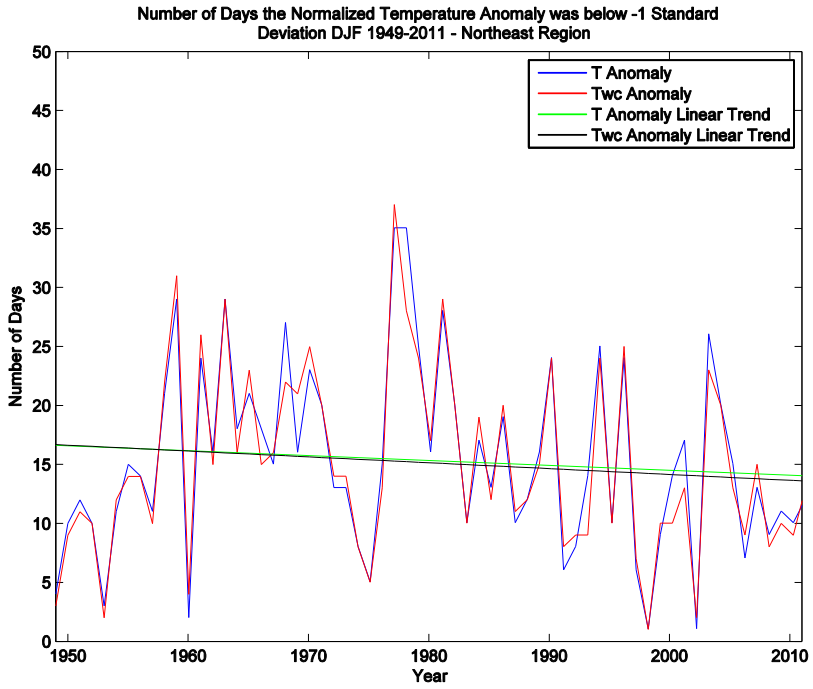

Figure 32: Number of Days the Normalized Temperature Anomaly was below -1σ for the Northeast Region, DJF 1949-2011

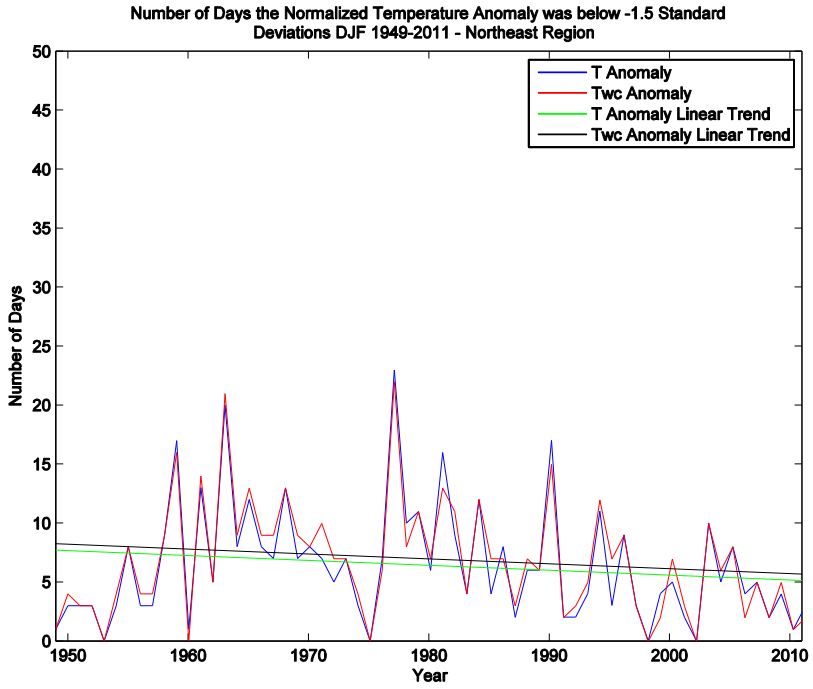

Figure 33: Number of Days the Normalized Temperature Anomaly was below -1.5σ for the Northeast Region, DJF 1949-2011

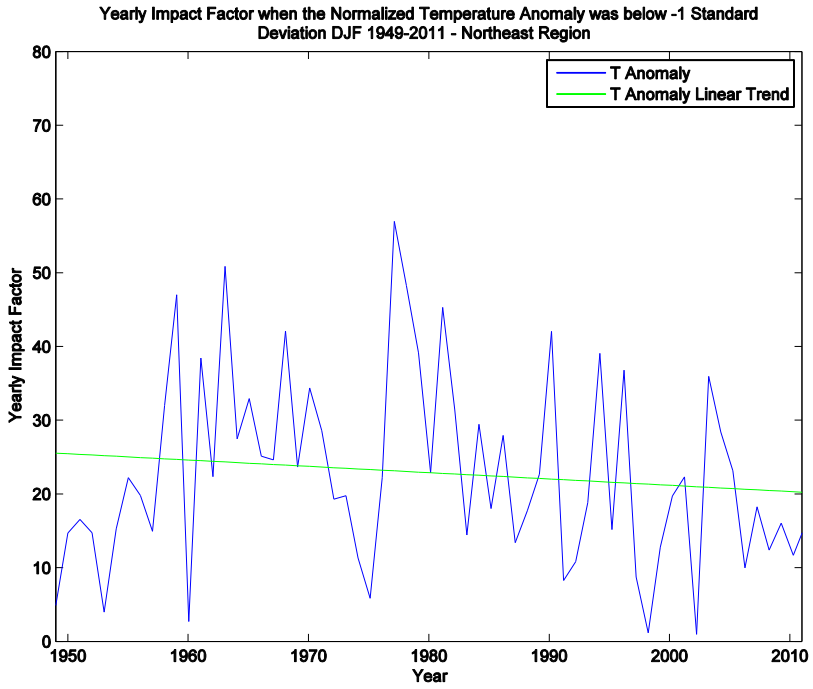

Figure 34: Impact Factor for Days the Normalized Temperature Anomaly was below -1σ for the Northeast Region, DJF 1949-2011

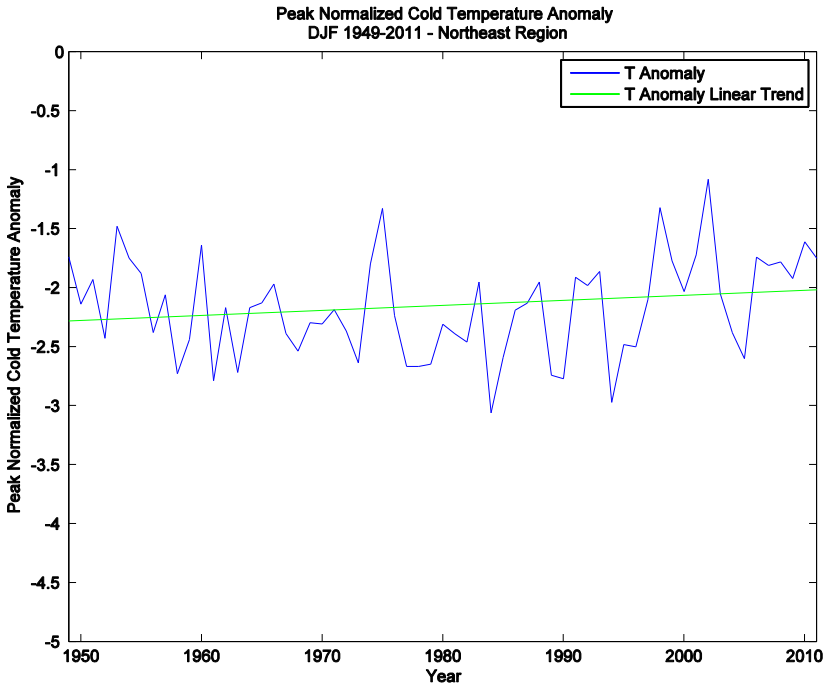

Figure 35: Peak Value for Days the Normalized Temperature Anomaly was below -1σ for the Northeast Region, DJF 1949-2011

On a related note, a recent study by Hankes and Walsh (2011) found that the number of extreme cold air mass events in the sub-arctic of North America, a source region for the cold air masses responsible for many of the CAOs that occur in the continental United States, has dramatically decreased over the past several decades. In addition, the temperatures within these extreme cold air masses have increased. It seems plausible, then, that changes observed in the source regions of CAOs should also be observed to some extent in the regions affected by the CAOs themselves. Paradoxically, however, these changes in extreme cold air masses in the sub-arctic have *not* translated into a parallel change in CAO frequency or amplitude in the midlatitudes of the United States, based on the results of this analysis as well as previous research (e.g. Walsh et al. 2001 and Portis et al. 2006) on CAO behavior.

To demonstrate that this method of identifying and analyzing ETRs is applicable to and valid using other datasets, the impact factor trend analysis for the SE region was re-performed for ETRs exceeding a temperature anomaly threshold of $\pm 1\sigma$ using MERRA data. Comparisons of the impact factor time series using MERRA data (red line) and NCEP/NCAR data (blue line) from 1979-2011 are shown in Figures 36 and 37. Overall, there is good correspondence between the two time series from 1979-2011 for both WWs and CAOs. The slight differences between the two time series are most likely a result of slight differences in the temperature and standard deviation climatologies. If a linear trend line is fit to the MERRA impact factor time series in Figures 36 and 37 (not shown) and the significance tested, neither of the trends was found to be significant at the 95% confidence level. In short, the trend analysis using MERRA data indicates that there has been no systematic increase or decrease in either WWs or CAOs in the SE region from 1979-2011. However, note that these trends using MERRA data cannot be directly compared to the trends using NCEP/NCAR data due to differences in the length of each dataset.

Therefore, the identification of ETRs using this method can theoretically be applied to other datasets and should achieve similar results to those shown here. However, whether or not the accompanying trend analysis will achieve similar results will depend upon the lengths of the datasets.

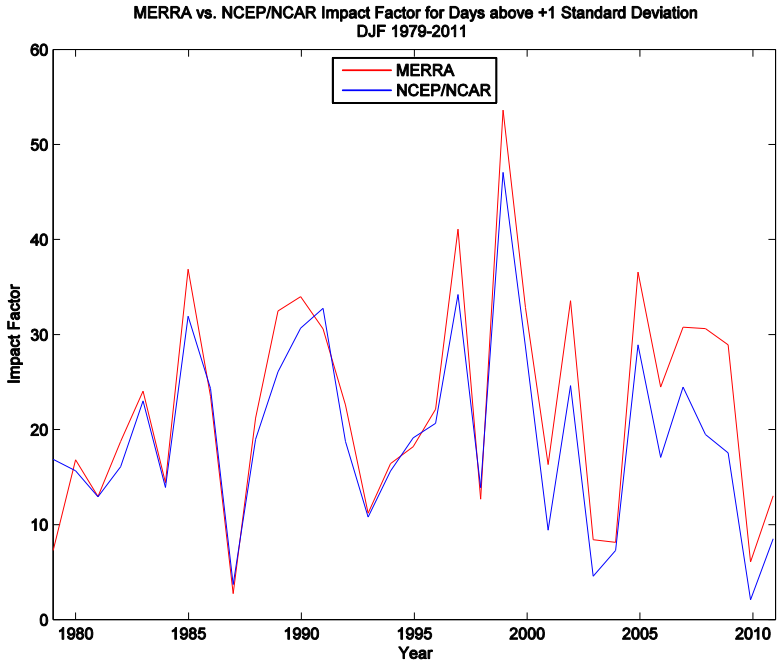

Figure 36: Comparison of the Impact Factor for Days above +1σ between MERRA and NCEP/NCAR data for the Southeast Region, DJF 1979-2011

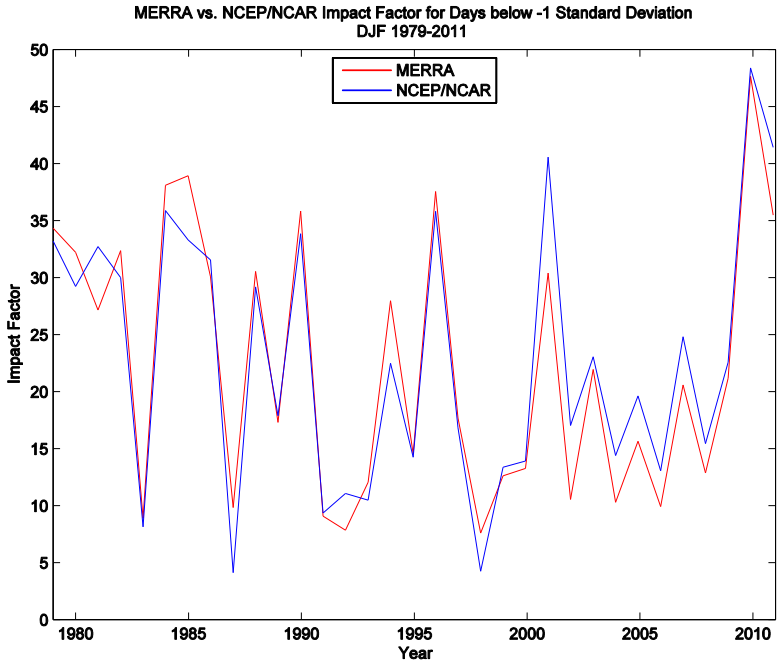

Figure 37: Comparison of the Impact Factor for Days below -1σ between MERRA and NCEP/NCAR data for the Southeast Region, DJF 1979-2011

The final aspect examined in this trend analysis was the Top 25 Cold and Warm Events for each region (Tables 2-4). The aim of this portion of the analysis was to identify the strongest ETR events from 1948-2011 using both T' and Twc'. These lists of events were created by ranking the peak value time series for days above or below ±1σ for each region from most extreme to least extreme. If more than one top event occurred in one winter season, each of the events must be separated by at least 7 days, the typical timescale of ETR events. In general, most of the strongest ETR events are identified by both T' and Twc' criterion; however, many of the events are ranked slightly differently depending on which criterion is used for event identification. For example, a CAO event that occurred in the MW region on February 21, 1963 is ranked seventh using T', whereas it is ranked fourth when Twc' is used. Likewise, a WW event that occurred in the SE region on January 7, 1998 was ranked ninth using T', while it was ranked eighth using Twc'. Therefore, there is a slight reordering of events when using Twc' to

identify extreme ETR events instead of T'. In addition, the spatial extent of some of the most extreme CAO and WW events is also evident in Tables 2-4. For instance, a CAO event near Christmas 1983 is the number one cold event for each region (except for the MW region using Twc', where it is ranked number two). Another example is a WW event that occurred during December 1998 and impacted all three regions. Interestingly, however, this event was ranked very differently in each region. It was ranked third (T') or fifth (Twc') for the MW region, fifth (T') or eighth (Twc') for the SE region, and seventh (T' and Twc') for the NE region.

Table 2: Top 25 Cold and Warm Events for the Midwest Region, 1949-2011

	Cold		Warm	
Event #	T'	Twc'	T'	Twc'
1	19-Dec-83	10-Jan-82	19-Feb-94	5-Dec-01
2	3-Feb-96	24-Dec-83	5-Dec-01	15-Feb-54
3	22-Dec-89	22-Dec-89	3-Dec-51	4-Dec-98
4	15-Jan-72	21-Feb-63	15-Feb-54	19-Feb-94
5	10-Jan-82	20-Jan-85	3-Dec-98	3-Dec-51
6	7-Dec-72	3-Feb-96	18-Feb-81	27-Dec-59
7	21-Feb-63	18-Jan-94	26-Feb-00	18-Feb-81
8	18-Jan-94	15-Jan-72	5-Dec-60	7-Jan-08
9	20-Jan-85	23-Jan-63	4-Dec-61	18-Jan-73
10	12-Dec-62	28-Jan-66	27-Dec-59	3-Dec-82
11	16-Dec-51	12-Dec-62	18-Jan-73	4-Dec-61
12	28-Jan-66	2-Dec-66	31-Dec-65	31-Dec-65
13	10-Dec-77	16-Dec-51	3-Dec-82	5-Dec-60
14	23-Jan-63	10-Dec-95	11-Feb-99	26-Feb-00
15	7-Jan-68	16-Jan-77	23-Jan-67	2-Dec-62
16	25-Feb-67	7-Jan-68	16-Dec-84	23-Jan-67
17	2-Dec-66	21-Feb-68	7-Jan-08	11-Feb-99
18	9-Dec-58	18-Feb-06	9-Feb-66	16-Dec-84
19	17-Feb-58	22-Feb-65	2-Dec-62	17-Jan-90
20	29-Jan-65	7-Dec-72	10-Feb-09	3-Dec-99
21	16-Jan-77	24-Feb-67	1-Dec-70	1-Dec-70
22	14-Dec-85	10-Dec-77	21-Dec-67	30-Jan-88
23	11-Dec-88	14-Dec-85	31-Dec-04	9-Feb-66
24	18-Dec-75	18-Dec-75	23-Dec-57	21-Dec-67
25	25-Feb-03	9-Dec-58	12-Feb-84	20-Feb-83

Table 3: Top 25 Cold and Warm Events for the Southeast Region, 1949-2011

	Cold		Warm	
Event #	**T'**	**Twc'**	**T'**	**Twc'**
1	25-Dec-83	25-Dec-83	3-Dec-82	3-Dec-82
2	21-Jan-85	21-Jan-85	1-Jan-52	1-Jan-52
3	23-Dec-89	23-Dec-89	25-Jan-50	6-Dec-98
4	13-Dec-62	13-Dec-62	25-Dec-82	25-Jan-50
5	17-Feb-58	30-Jan-66	6-Dec-98	25-Dec-82
6	4-Feb-96	17-Feb-58	31-Dec-51	30-Dec-84
7	11-Jan-82	11-Jan-82	7-Dec-51	14-Dec-48
8	30-Jan-66	4-Feb-96	15-Dec-48	7-Jan-98
9	17-Jan-77	25-Feb-67	7-Jan-98	7-Dec-51
10	25-Feb-67	17-Jan-77	21-Dec-67	21-Dec-67
11	12-Dec-57	12-Feb-55	22-Jan-99	31-Jan-02
12	11-Jan-62	24-Jan-63	30-Dec-84	14-Feb-59
13	9-Jan-70	9-Jan-70	15-Dec-71	9-Feb-57
14	26-Dec-85	12-Dec-57	14-Feb-59	24-Jan-49
15	28-Jan-86	11-Jan-62	31-Jan-02	27-Jan-52
16	19-Jan-94	24-Jan-03	29-Jan-75	29-Jan-75
17	24-Jan-03	2-Feb-51	9-Feb-57	14-Jan-60
18	24-Jan-63	26-Dec-85	24-Jan-49	31-Dec-96
19	12-Feb-55	24-Feb-89	27-Jan-52	22-Jan-99
20	16-Dec-51	16-Dec-51	13-Jan-05	1-Jan-85
21	20-Dec-00	19-Jan-94	30-Dec-90	15-Dec-71
22	22-Feb-63	28-Jan-86	1-Jan-85	30-Dec-90
23	24-Feb-89	22-Feb-63	2-Jan-66	23-Dec-56
24	16-Feb-91	7-Feb-78	2-Feb-74	3-Feb-90
25	2-Feb-51	16-Feb-91	4-Jan-97	2-Feb-74

Table 4: Top 25 Cold and Warm Events for the Northeast Region, 1949-2011

	Cold		Warm	
Event #	T'	Twc'	T'	Twc'
1	25-Dec-83	25-Dec-83	26-Jan-50	26-Jan-50
2	19-Jan-94	17-Feb-58	15-Jan-95	15-Jan-95
3	13-Dec-60	19-Jan-94	29-Dec-84	9-Dec-66
4	22-Dec-89	31-Dec-62	9-Dec-66	4-Dec-82
5	12-Dec-88	13-Dec-60	4-Dec-82	6-Jan-07
6	17-Feb-58	21-Jan-85	6-Jan-07	29-Dec-84
7	22-Feb-63	22-Dec-89	7-Dec-98	7-Dec-98
8	31-Dec-62	11-Jan-82	20-Dec-57	16-Feb-54
9	3-Dec-76	22-Feb-63	6-Dec-01	6-Dec-01
10	11-Dec-77	17-Feb-79	26-Dec-82	25-Jan-67
11	17-Feb-79	25-Feb-67	25-Jan-67	25-Dec-82
12	17-Feb-73	6-Feb-95	16-Feb-54	19-Feb-81
13	20-Dec-04	17-Feb-73	25-Dec-64	20-Dec-57
14	21-Jan-85	17-Jan-77	19-Feb-81	25-Dec-64
15	8-Jan-68	20-Dec-04	24-Feb-85	24-Feb-85
16	5-Feb-96	16-Dec-51	5-Jan-07	22-Dec-90
17	17-Jan-77	13-Dec-62	22-Dec-90	8-Jan-08
18	6-Feb-95	8-Jan-68	8-Jan-08	6-Jan-98
19	13-Dec-62	3-Dec-76	7-Dec-51	7-Dec-51
20	11-Jan-82	25-Dec-80	20-Feb-94	7-Dec-56
21	11-Dec-58	10-Jan-78	22-Jan-57	26-Feb-57
22	16-Dec-51	20-Feb-59	27-Jan-74	5-Dec-73
23	26-Feb-90	4-Jan-81	5-Dec-73	20-Feb-94
24	20-Feb-59	21-Feb-68	26-Feb-57	19-Jan-86
25	31-Jan-48	6-Jan-59	28-Dec-08	5-Jan-97

3.2 Correlation Analysis

The correlation analysis results revealed several significant associations between the regional ETR metrics for events exceeding a threshold of ±1σ and several prominent low frequency modes (Tables 5-7). The significant correlations are highlighted in blue if the p-value was less than 0.05 and in green if the p-value was was less than 0.10. If the ETR metric is positively (negatively) correlated with a particular low frequency mode, then that ETR metric tends to be higher when that low frequency mode is in its positive (negative) phase. Generally,

the results in Tables 5-7 indicate that ETRs in each region tend to be modulated by certain low frequency modes.

In the SE region, there is a significant correlation between the ETR metrics for WWs and the low frequency mode indices for the AO, NAO, PNA, PDO, MEI, Nino 3.4 and SOI (Table 5). Therefore, WWs are more likely to occur in the SE region when the AO, NAO, and SOI are in their positive phases and when the PNA, PDO, MEI and Nino 3.4 are in their negative phases. On the other hand, there is a significant association between the ETR metrics for CAOs and the AO, NAO, and PDO indices (Table 5). Thus, CAOs are more likely to occur in the SE region when the AO and NAO are in their negative phases and when the PDO is in its positive phase. These results are consistent with the conclusions of previous studies (e.g. Walsh et al. 2001 and Cellitti et al. 2006) that CAOs over the United States are linked to the negative phases of the AO and NAO. Additionally, it is interesting that seven different low frequency modes are significantly correlated with the ETR metrics for WWs, while only three different low frequency modes are significantly correlated with the ETR metrics for CAOs. Thus, there is an apparent asymmetry in the low frequency mode modulation on ETRs in the SE region.

In the MW region, there is a significant correlation between the ETR metrics for WWs and the low frequency mode indices for the AO, NAO, and PNA (Table 6). Thus, WWs are more likely to occur in the MW region when the AO, NAO, and PNA are in their positive phases. Interestingly, however, there are no significant correlations between the ETR metrics for CAOs and the low frequency mode indices. Therefore, it appears that there is an asymmetry in the low frequency mode modulation on ETRs for the MW region as well.

In the NE region, there is a significant correlation between the ETR metrics for WWs and the low frequency mode indices for the AO, NAO, and PDO (Table 7). As a result, WWs are

more likely to occur in the NE region when the AO or NAO is in its positive phase and the PDO is in its negative phase. On the other hand, there is a significant association between the ETR metrics for CAOs and the AO index (Table 7). Thus, CAOs in the NE region are more likely when the AO is in its negative phase, which is consistent with the findings of previous studies (e.g. Walsh et al. 2001 and Cellitti et al. 2006) that CAOs over the United States are associated with the negative phase of the AO. In addition, notice how three different low frequency modes are significantly correlated with the ETR metrics for WWs, while only one low frequency mode is significantly correlated with the ETR metrics for CAOs. Thus, it is evident that there is an asymmetry in the low frequency mode modulation of ETRs in the NE region as well.

Table 5: Correlation Values for the Southeast Region*, 1950-2011

SE Region Correlations	Number of Cold Days	Number of Warm Days	Cold Days Impact Factor	Warm Days Impact Factor	Cold Days Peak Amplitude	Warm Days Peak Amplitude
Seasonal Mean AO Index	-0.48	0.45	-0.47	0.43	0.20	0.36
Seasonal Mean NAO Index	-0.51	0.41	-0.49	0.40	0.20	0.33
Seasonal Mean PNA Index	0.27	-0.60	0.26	-0.59	-0.01	-0.38
Seasonal Mean PDO Index	0.32	-0.63	0.32	-0.60	-0.20	-0.40
Seasonal Mean MEI Index	0.08	-0.46	0.07	-0.44	0.11	-0.22
Seasonal Mean Nino 3.4 Index	0.06	-0.45	0.05	-0.43	0.12	-0.25
Seasonal Mean SOI Index	-0.01	0.31	-0.01	0.28	-0.13	0.09
NPGO	0.25	-0.30	0.23	-0.29	0.03	-0.24
AMO	-0.12	-0.11	-0.13	-0.11	0.17	0.04

* blue (green) shading indicates significance at the 95% (90%) confidence level

Table 6: Correlation Values for the Midwest Region*, 1950-2011

MW Region Correlations	Number of Cold Days	Number of Warm Days	Cold Days Impact Factor	Warm Days Impact Factor	Cold Days Peak Amplitude	Warm Days Peak Amplitude
Seasonal Mean AO Index	-0.24	0.40	-0.23	0.39	-0.04	0.14
Seasonal Mean NAO Index	-0.22	0.41	-0.22	0.40	-0.01	0.23
Seasonal Mean PNA Index	-0.06	0.28	-0.05	0.27	0.17	0.06
Seasonal Mean PDO Index	0.08	0.10	0.11	0.08	-0.08	-0.05
Seasonal Mean MEI Index	-0.13	0.24	-0.10	0.20	0.05	0.02
Seasonal Mean Nino 3.4 Index	-0.16	0.19	-0.13	0.15	0.08	0.01
Seasonal Mean SOI Index	0.15	-0.24	0.11	-0.20	0.01	-0.02
NPGO	-0.16	0.17	-0.18	0.18	0.29	0.01
AMO	-0.34	0.24	-0.34	0.25	0.42	0.19

* blue (green) shading indicates significance at the 95% (90%) confidence level

Table 7: Correlation Values for the Northeast Region*, 1950-2011

NE Region Correlations	Number of Cold Days	Number of Warm Days	Cold Days Impact Factor	Warm Days Impact Factor	Cold Days Peak Amplitude	Warm Days Peak Amplitude
Seasonal Mean AO Index	-0.30	0.56	-0.29	0.55	0.02	0.39
Seasonal Mean NAO Index	-0.29	0.51	-0.27	0.53	0.00	0.47
Seasonal Mean PNA Index	0.10	-0.24	0.10	-0.23	0.09	-0.11
Seasonal Mean PDO Index	0.24	-0.35	0.24	-0.34	-0.12	-0.17
Seasonal Mean MEI Index	0.03	-0.14	0.03	-0.11	-0.02	0.08
Seasonal Mean Nino 3.4 Index	0.01	-0.18	0.00	-0.15	0.02	0.02
Seasonal Mean SOI Index	-0.06	0.01	-0.06	-0.02	0.07	-0.12
NPGO	-0.05	-0.11	-0.08	-0.13	0.36	-0.25
AMO	-0.25	0.07	-0.24	0.05	0.30	-0.02

* blue (green) shading indicates significance at the 95% (90%) confidence level

Table 8: Correlation Values between Low Frequency Modes*, 1950-2011

	AO Seasonal Index	NAO Seasonal Index	PNA Seasonal Index	PDO Seasonal Index	MEI Seasonal Index	Nino 3.4 Seasonal Index	SOI Seasonal Index
AO Seasonal Index	1						
NAO Seasonal Index	0.7924	1					
PNA Seasonal Index	-0.189	0.0153	1				
PDO Seasonal Index	-0.2854	-0.0533	0.7476	1			
MEI Seasonal Index	-0.1151	-0.0483	0.4729	0.5372	1		
Nino 3.4 Seasonal Index	-0.1948	-0.1256	0.4386	0.4594	0.9633	1	
SOI Seasonal Index	0.0945	0.0328	-0.3925	-0.4734	-0.92	-0.8916	1

* blue shading indicates significance at the 95% confidence level

In addition to examining the correlations between the ETR metrics and several prominent low frequency modes, the correlations among the top seven prominent low frequency modes in Tables 5-7 were also examined (Table 8). It was found that the AO index is significantly correlated with the NAO index, while the PNA index is significantly correlated with the PDO, MEI and Nino 3.4 indices. Likewise, the PDO is significantly correlated with the MEI, Nino 3.4, and SOI indices, while the MEI is significantly correlated with the Nino 3.4 and SOI indices. Also, the Nino 3.4 index is significantly correlated with the SOI index. However, these significant correlations among the low frequency modes could be indicative of potential multicollinearities, where one low frequency mode index contains information on another low frequency mode index. Therefore, these significant correlations could have important potential impacts on the multiple linear regressions, which use these low frequency mode indices as predictors. However, this issue will be addressed further in Section 3.3.

To verify the results of the correlation analysis, correlations between surface air temperature (SAT) and several of the aforementioned low frequency modes were calculated and plotted using the NOAA/ESRL website (http://www.esrl.noaa.gov/psd/data/correlation/) and were compared to the significant correlation values in Tables 5-7. The seasonally averaged DJF surface air temperature was correlated with the seasonally averaged DJF low frequency mode indices for the AO, NAO, PNA, PDO, MEI and Nino 3.4 for the period 1950-2011. The SOI index was unavailable on the website at the time of writing. The resulting correlation plots for the AO, NAO, PNA, and PDO are shown in Figures 38-41, which are the four primary low frequency modes that had significant correlations in each of the regions of interest.

In general, there is good correspondance between the significant correlation values shown in Tables 5-7 and the correlation values in Figures 38-41. For the SE region in Figures 38 and 39, the AO and NAO indices are positively correlated with the SAT and have correlation coefficients ranging from 0.45 to 0.50, which are similar to the significant correlation values shown in Table 5. In Figures 40 and 41, the PNA and PDO indices are negatively correlated with the SAT in the SE region, and have a correlation coefficient of -0.55 to -0.60, which are also similar to the significant correlation values of the WW metrics in Table 5. However, the correlation coefficient for the PDO in Figure 41 is higher than the significant correlation value for the CAO metrics in Table 5. This is likely a result of the aforementioned asymmetry in the low frequency mode modulation of ETRs in this region. In addition, the correlation plots of the MEI and Nino 3.4 indices and the SAT (not shown) for the SE region had similar correlation values as those for the WW metrics in Table 5. For the Midwest region, the AO and NAO indices (Figures 38 and 39, respectively) are positively correlated with the SAT and have a correlation coefficient ranging from 0.30-0.40, while the PNA (Figure 40) is also positively correlated with the SAT and has an

average correlation coefficient of approximately 0.25. Both of these results are similar to the significant correlation values in Table 6. For the NE region, the AO and NAO (Figures 38 and 39, respectively) are positively correlated with the SAT and have a correlation coefficient ranging from 0.40-0.50, which match the significant correlation coefficients for the WW metrics in Table 7. However, the correlation coefficient for the AO index in Figure 38 is higher than the significant correlation value for the CAO metrics, and is most likely a result of the aforementioned asymmetry in the low frequency mode modulation of ETRs in this region. In addition, the PDO index (Figure 41) for the NE region is negatively correlated with the SAT and has an averaged correlation coefficient of approximately -0.30, which is similar to the significant correlation value for WWs in Table 7. Thus, overall, there appears to be good agreement between the significant correlation values in Tables 5-7 and the correlation patterns exhibited in Figures 38-41.

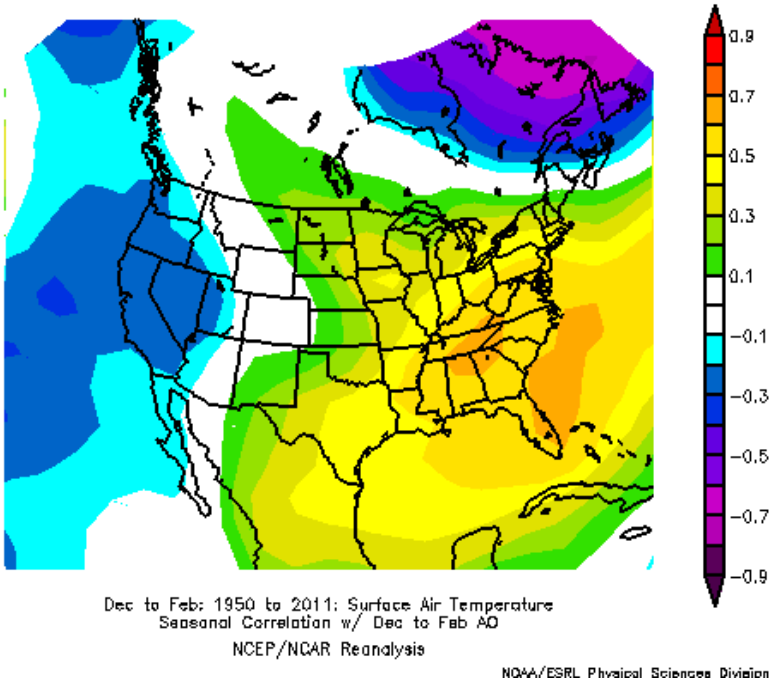

Figure 38: Correlation Plot of Surface Air Temperature and the DJF Seasonal Mean AO Index. Courtesy of NOAA/ESRL Physical Sciences Division.

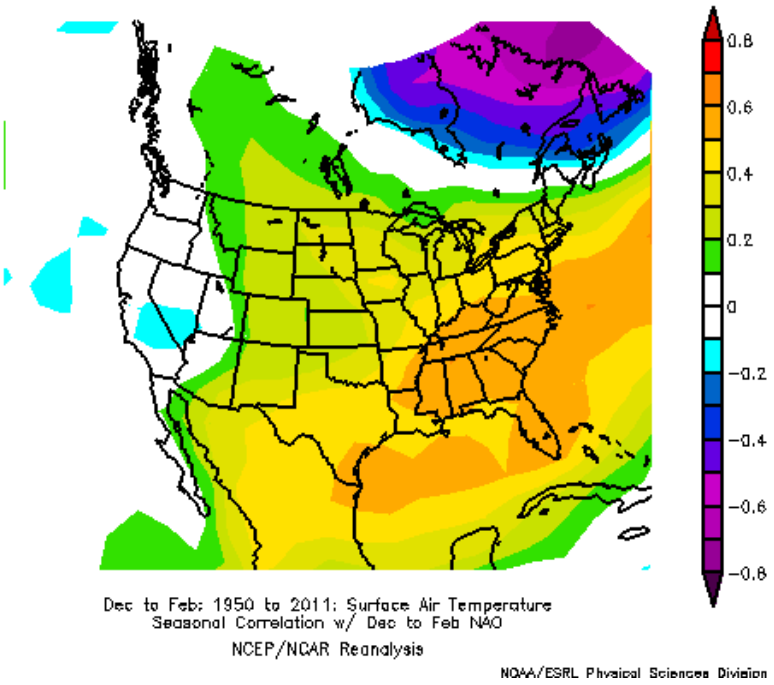

Figure 39: Correlation Plot of Surface Air Temperature and the DJF Seasonal Mean NAO Index. Courtesy of NOAA/ESRL Physical Sciences Division.

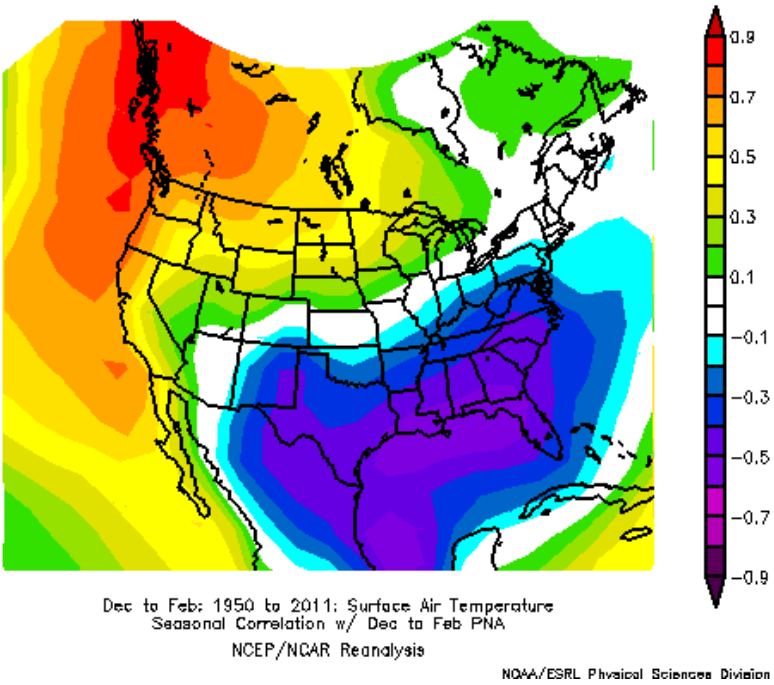

Figure 40: Correlation Plot of Surface Air Temperature and the DJF Seasonal Mean PNA Index. Courtesy of NOAA/ESRL Physical Sciences Division.

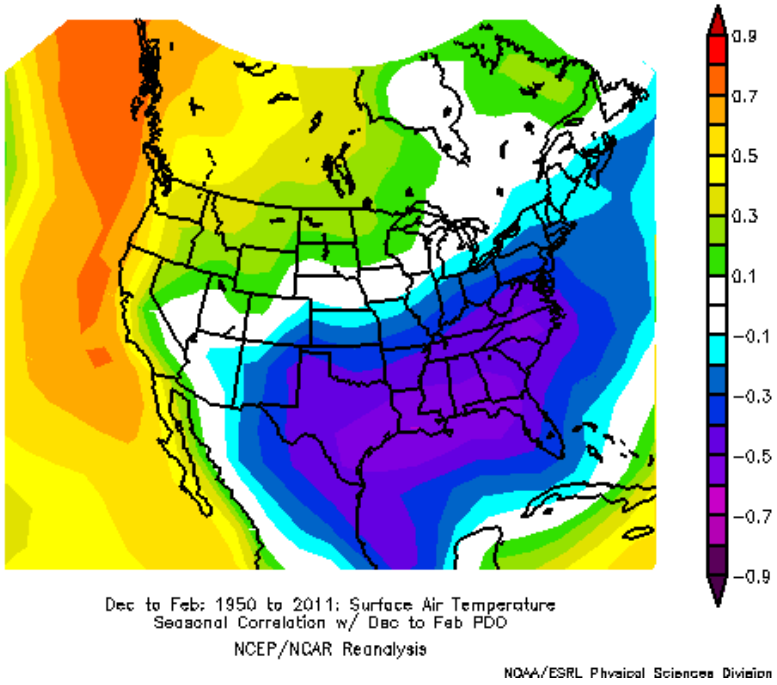

Figure 41: Correlation Plot of Surface Air Temperature and the DJF Seasonal Mean PDO Index. Courtesy of NOAA/ESRL Physical Sciences Division.

In summary, the results of the correlation analysis indicated that (1) ETRs in each region tend to be modulated by certain low frequency modes and (2) there is an apparent asymmetry between the low frequency modulation of CAOs and WWs. This asymmetry was highlighted by the fact that WWs in each region are significantly correlated with at least three low frequency modes, while CAOs are significantly correlated with three or less low frequency modes. Based on these findings, it appears that it may be easier to explain WW modulation by low frequency modes than it is to explain CAO modulation. Interestingly, this is in contrast with recent findings by Guirguis et al. (2010), who found that the low frequency modes did not account for warm extremes nearly as well as cold extremes in the Northern Hemisphere. However, those results are generalized for the entire Northern Hemisphere, and perhaps may not be directly applicable to the specific regions used in this analysis.

There are a few speculative explanations for the apparent asymmetry in the low frequency mode modulation of CAOs and WWs. First, the absence of significant CAO modulation by low frequency modes in the MW region could be due to geographical location. If this region is located at or near the node of a particular low frequency mode, the effect of that particular low frequency mode on CAOs will likely be minimal, since the location of the positive and negative cells of a particular low frequency mode will determine whether zonal flow or meridional flow is prominent. Meridional flow is the type required for the temperature advection effect that is characteristic of WWs and CAOs, and there will not likely be any substantial meridional flow if the region is located between the two cells of the low frequency mode. However, this explanation is purely speculative at this point and could be verified by analyzing the low frequency mode circulation patterns in further detail. Second, the apparent asymmetry between the low frequency mode modulation of CAOs and WWs could also be due to the intrinsic non-linearity in differences of the low frequency mode phases. It has traditionally been assumed that the atmospheric climate reactions associated with the positive and negative phases of various low frequency modes are equal and opposite of each other, and hence assume a linear relationship. Recently, however, both observational studies and numerical models have shown that the North American climate has an asymmetric response pattern during the opposite phases of ENSO (Wu et al. 2005) and the AO (Wu et al. 2006). However, this is yet another conjecture that should be verified, using composite analyses of the opposing phases of these low frequency modes, and applied to other low frequency modes as well.

3.3 Multiple Linear Regression Analysis

Using the results of the correlation analysis, multiple linear regressions were performed to assess how much of the interannual variability in the ETR metrics can be explained by various combinations of the significantly correlated low frequency modes and to determine which combination of low frequency modes explains the maximum amount of variance. However, when using multiple linear regressions, there are two important considerations: (1) potential multicollinearities and (2) autocorrelation in the residuals. Testing for multicollinearity is important because it isn't always known a priori whether one predictor contains redundant information in relation to another predictor. Testing for autocorrelation in the residuals is equally important because autocorrelation in the residuals degrades the regression and its associated statistics. Therefore, accounting for existing autocorrelation in the residuals will allow for accurate statistical conclusions.

To determine whether multicollinearity is an issue among the predictors used for the multiple linear regressions, the Belsley-Kuh-Welsch (BKW) variance-decomposition method was applied, as described by Belsley, Kuh, and Welsch (1980). If any multicollinearities were detected among the predictors, only one of the multicollinear predictors was used in the regression. To determine which of the predictors in the multicollinear subset would be used in the regression, each multicollinear predictor was regressed individually onto the ETR metric time series and the output statistics were examined. The multicollinear predictor that had a combination of statistically significant p-values and the highest r-squared value was chosen as one of the predictors to be used in the regression. Accordingly, this process created a smaller subset of predictors for the multiple linear regression that did not contain multicollinearity.

After the multiple linear regression equation that produced the best fit to the ETR metric time series was identified, the Durbin-Watson (DW) statistic was calculated to test for autocorrelation in the residuals. If the p-value for DW statistic was below 0.05, autocorrelation in the residuals was present and the multiple linear regression was re-performed using the Cochrane-Orcutt (CO) method. Before deciding upon the CO method, one other method was attempted to account for and remove the autocorrelation in the residuals. This method added another predictor in the regression equation, informally named the "autocorrelation term", that was related to the previous year's ETR metric. This method was successful in removing the autocorrelation in the residuals, as determined by the DW statistic. Curiously, however, the regression estimates of the time series including the "autocorrelation term" were virtually identical to the regression estimates of the time series not including the "autocorrelation term". Therefore, due to this uncertainty, and because the CO method was developed specifically to account for autocorrelation in the residuals, the CO method was selected.

The results of the multiple linear regression analysis are exhibited in Table 9, which lists the optimal combination of predictors that explains the maximum amount of variance for each ETR metric and the associated variance explained. The best combination of predictors was not limited to a specific number of predictors. However, it turns out that a combination of two predictors explains the maximum amount of variance in the ETR metrics in many of the cases. This occurred purely by chance and was entirely determined by the statistics. In the MW region, the best combination of predictors for the WW metrics incorporated the AO and PNA indices, and accounts for nearly 30% of the variance. For the SE region, the combination of the AO and PDO indices explains nearly 50% of the variability in the WW metrics, except for the warm days peak amplitude metric, where only 22% of the variance is explained. On the other hand, the

combination of the NAO and PDO indices accounts for nearly 30% of the variance in the ETR time series for CAOs in the SE region. In the NE region, the best combination of predictors consisted of the NAO and PDO indices, which account for approximately 30% of the variance in WWs in the NE region. However, for the warm days peak amplitude, the best predictor is the NAO index, which accounts for about 22% of the variance. On the other hand, the AO index alone is the best (and only) predictor for CAO metrics in the NE region, and explains approximately 10% of the variance.

For visual illustration of how well the multiple linear regressions can represent the ETR time series, plots of the Number of Days T' was above +1σ (Y) versus the multiple linear regression estimate (Yhat) for the SE and NE regions are shown in Figures 42 and 43, respectively. In general, there is good correspondence between Y and Yhat for each region and the regression estimate recreates the interannual variability in the time series quite well. Of the two regions shown, the best correspondence between Y and Yhat is in the SE region, but this is because more of the variance in the ETR time series is explained by the low frequency modes in that region than in the NE region (Table 9).

Table 9: The Best Combination of Predictors and Maximum Variance Explained for each ETR metric 1950-2011

Region	Metric	Best Combination of Predictors	Variance Explained
MW	Number of Cold Days	--	--
	Number of Warm Days	AO & PNA	29.57%
	Cold Days Impact Factor	--	--
	Warm Days Impact Factor	AO & PNA	27.79%
	Cold Days Peak Amplitude	--	--
	Warm Days Peak Amplitude	--	--
SE	Number of Cold Days	NAO & PDO	28.05%
	Number of Warm Days	AO & PDO	47.91%
	Cold Days Impact Factor	NAO & PDO	27.81%
	Warm Days Impact Factor	AO & PDO	43.93%
	Cold Days Peak Amplitude	--	--
	Warm Days Peak Amplitude	AO & PDO	22.06%
NE	Number of Cold Days	AO	9.24%
	Number of Warm Days	NAO & PDO	30.55%
	Cold Days Impact Factor	AO	8.14%
	Warm Days Impact Factor	NAO & PDO	33.68%
	Cold Days Peak Amplitude	--	--
	Warm Days Peak Amplitude	NAO	21.85%

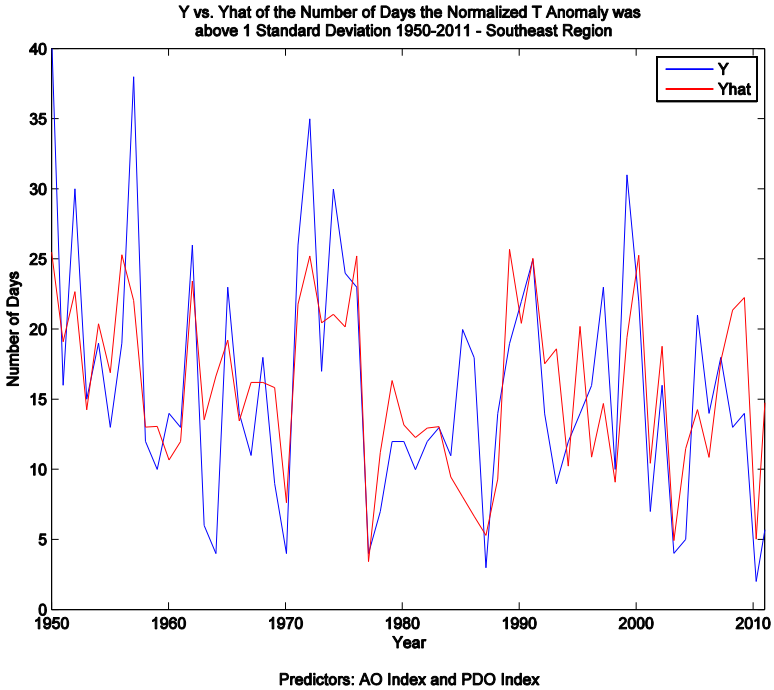

Figure 42: Y vs. Yhat of the Number of Days the Normalized T Anomaly was above +1σ for the Southeast Region, 1950-2011

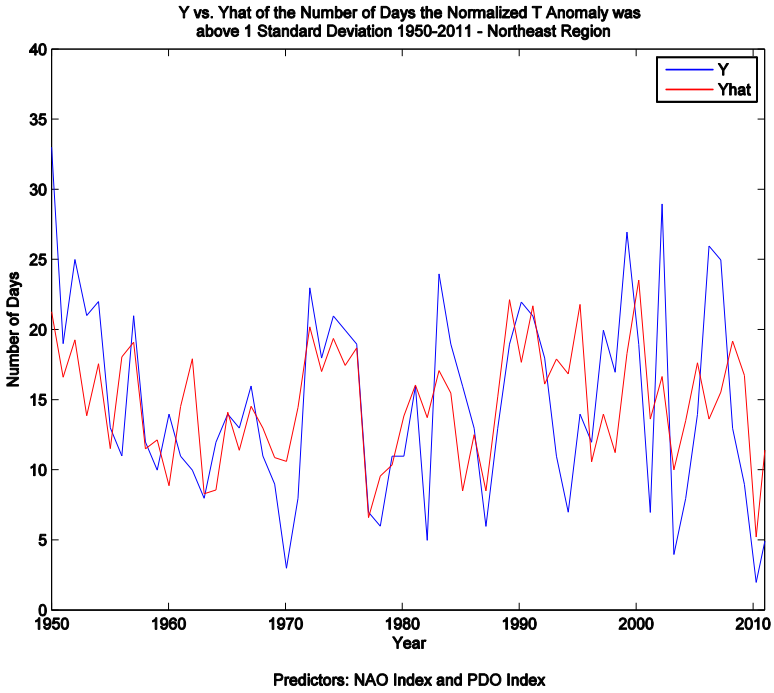

Figure 43: Y vs. Yhat of the Number of Days the Normalized T Anomaly was above +1σ for the Northeast Region, 1950-2011

Overall, various combinations of low frequency modes in each of the three regions of interest explain anywhere between 10% and 50% of the variance in the ETR metrics, and are therefore not able to completely reproduce the interannual variability observed in the ETR metric time series. The variability that is left unaccounted for by the multiple linear regressions could be cause by a large variety of things, including local or regional effects such as the land-sea distribution, other low frequency modes that are not considered in this analysis, or simply just random variability. Nonetheless, these results may still be useful in applications of assessing risk and forecasting these events on a seasonal basis.

Chapter 4

Conclusions

During the boreal cool season, extreme temperature regimes (ETRs), including cold air outbreaks (CAOs) and warm waves (WWs), affect regional economies and human safety over large portions of the United States via their significant impacts on energy consumption, local agriculture, and human health. The present study (1) examines the trends in frequency and amplitude of ETRs and (2) determines and quantifies how these behaviors in ETRs are modulated by low frequency modes. This was pursued by applying a range of statistical analyses to observational reanalysis data, including trend, correlation and multiple linear regression analyses.

First, the regional long-term variability analysis reveals that there has been a statistically significant decrease in the frequency and amplitude of boreal cool season WWs over the SE US from 1949-2011, but no statistically significant trends in WWs or CAOs are found for any other region. Therefore, there has *not* been any significant reduction in either the amplitude or frequency of CAOs over the eastern United States from 1949-2011. In fact, the recent winters of 2009/2010 and 2010/2011 both rank among the top 5 coldest winters in terms of CAO metrics for the SE region (Figures 24-26). In addition, strong interannual variability in ETRs is evident from 1949-2011 in each region. Therefore, it is likely that ETRs will continue to occur just as often in the near future as they have in the past, even with a concurrently changing background climate. The results of the correlation analysis indicate that ETRs in each region are strongly modulated by certain low frequency modes, with asymmetries between the low frequency mode modulation of CAOs and WWs, while the multiple linear regression analysis reveals that various

combinations of low frequency modes can explain anywhere between 10% and 50% of the variance in the ETR metrics. If this newfound information is incorporated into the regional forecasts of these events, the forecasts for WWs and CAOs will likely be significantly improved.

Extreme temperature regimes will remain an interest to weather forecasters because of their socioeconomic impacts. Based on the results of this research, particularly the lack of trends in historical ETR variability, ETRs may occur just as frequently and intensely as they have over the past 60 years. Therefore, accurate prediction and forecasting of these events is desirable. Additionally, the fact that the frequency and amplitude of ETRs in the United States has not changed, even with increasing background temperatures, provides impetus for identifying and understanding the dynamical mechanisms responsible for ETRs. Therefore, it is necessary to better understand the synoptic and dynamic processes responsible for ETRs and their low frequency modulation. Several studies have examined the cold air outbreak process synoptically via a thermodynamic perspective (e.g. Konrad and Colucci 1989), but attention to the dynamical mechanisms that trigger the outbreak itself by facilitating the latitudinal transport of air masses remains an important, yet little understood, concept. Furthermore, there is little existing research on the physical nature of boreal cool season WWs. Investigating these dynamical triggers and their corresponding circulations will have relevant applications to forecasting ETRs by providing further valuable scientific insight and understanding, thereby leading to improved forecasts helping to reduce the negative impacts associated with these events. Finally, a more complete physical understanding of ETR mechanisms is essential for elucidating likely future variability in association with climate change.

References

Belsley, D. A., E. Kuh, and R. E. Welsch, 1980: *Regression Diagnostics: Identifying Influential Data and Sources of Collinearity.* John Wiley & Sons, 292 pp.

Cellitti, M. P., J. E. Walsh, R. M. Rauber, and D. H. Portis, 2006: Extreme cold air outbreaks over the United States, the polar vortex, and the large-scale circulation. *Journal of Geophysical Research*, **111,** 14p.

Cohen, J., J. Foster, M. Barlow, K. Saito, and J. Jones, 2010: Winter 2009–2010: A case study of an extreme Arctic Oscillation event. *Geophysical Research Letters*, **37,** 161-168.

Downton, M. W., and K. A. Miller, 1993: The Freeze Risk to Florida Citrus. Part II: Temperature Variability and Circulation Patterns. *Journal of Climate*, **6,** 364-372.

Easterling, D. R., J. L. Evans, P. Y. Groisman, T. R. Karl, K. E. Kunkel, and P. Ambenje, 2000: Observed Variability and Trends in Extreme Climate Events: A Brief Review. *Bulletin of the American Meteorological Society*, **81,** 417-425.

Gu, L., and Coauthors, 2008: The 2007 Eastern US Spring Freeze: Increased Cold Damage in a Warming World. *BioScience*, **58,** 253.

Guirguis, K., A. Gershunov, R. Schwartz, and S. Bennett, 2011: Recent warm and cold daily winter temperature extremes in the Northern Hemisphere. *Geophysical Research Letters*, **38,** 6p.

Hankes, I. E., and J. E. Walsh, 2011: Characteristics of extreme cold air masses over the North American sub-Arctic. *Journal of Geophysical Research*, **116**.

Kalnay, E., et al., 1996: The NCEP/NCAR 40-Year Reanalysis Project. *Bulletin of the American Meteorological Society*, **77,** 437-471.

Konrad, C. E., and S. J. Colucci, 1989: An Examination of Extreme Cold Air Outbreaks over Eastern North America. *Monthly Weather Review*, **117,** 2687-2700.

Osczevski, R., and M. Bluestein, 2005: The New Wind Chill Equivalent Temperature Chart. *Bulletin of the American Meteorological Society*, **86,** 1453-1458.

Park, T.-W., C.-H. Ho, S.-J. Jeong, Y.-S. Choi, S. K. Park, and C.-K. Song, 2011: Different characteristics of cold day and cold surge frequency over East Asia in a global warming situation. *Journal of Geophysical Research*, **116**.

Portis, D. H., M. P. Cellitti, W. L. Chapman, and J. E. Walsh, 2006: Low-Frequency Variability and Evolution of North American Cold Air Outbreaks. *Monthly Weather Review*, **134,** 579-597.

Rogers, J. C., and R. V. Rohli, 1991: Florida Citrus Freezes and Polar Anticyclones in the Great Plains. *Journal of Climate*, **4,** 1103-1113.

Suarez, M. J., et al, 2008: The GEOS-5 Data Assimilation System - Documentation of Versions 5.0.1, 5.1.0, and 5.2.0. *NASA Technical Report Series on Global Modeling and Data Assimilation*, **27,** 118.

Walsh, J. E., A. S. Phillips, D. H. Portis, and W. L. Chapman, 2001: Extreme Cold Outbreaks in the United States and Europe, 1948-99. *Journal of Climate*, **14,** 2642-2658.

Vavrus, S., J. E. Walsh, W. L. Chapman, and D. Portis, 2006: The behavior of extreme cold air outbreaks under greenhouse warming. *International Journal of Climatology*, **26,** 1133-1147.

Wang, C., H. Liu, and S.-K. Lee, 2010: The record-breaking cold temperatures during the winter of 2009/2010 in the Northern Hemisphere. *Atmospheric Science Letters*, **11,** 161-168.

Wheeler, D. D., V. L. Harvey, D. E. Atkinson, R. L. Collins, and M. J. Mills, 2011: A climatology of cold air outbreaks over North America: WACCM and ERA-40 comparison and analysis. *Journal of Geophysical Research*, **116**.

Wilks, D. S., 2006: *Statistical Methods in the Atmospheric Sciences.* Second ed. Elsevier, 627 pp.

Wu, A., W. W. Hsieh, and A. Shabbar, 2005: The Nonlinear Patterns of North American Winter Temperature and Precipitation Associated with ENSO. *Journal of Climate*, **18,** 1736-1752.

Wu, A., W. W. Hsieh, A. Shabbar, G. J. Boer, and F. W. Zwiers, 2006: The nonlinear association between the Arctic Oscillation and North American winter climate. *Climate Dynamics*, **26,** 865-879.